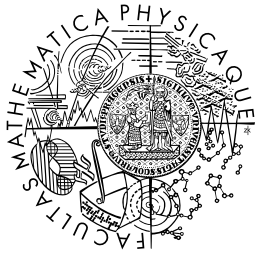

FACULTY
OF MATHEMATICS
AND PHYSICS
Charles University

BACHELOR THESIS

Matyáš Bílek

Continuous and distributional description of impulsive gravitational waves

Institute of Theoretical Physics

Supervisor of the bachelor thesis: doc. RNDr. Robert Švarc, Ph.D.
Study programme: Physics (B0533A110001)

Prague 2024

I declare that I carried out this bachelor thesis independently, and only with the cited sources, literature and other professional sources. It has not been used to obtain another or the same degree.

I understand that my work relates to the rights and obligations under the Act No. 121/2000 Sb., the Copyright Act, as amended, in particular the fact that the Charles University has the right to conclude a license agreement on the use of this work as a school work pursuant to Section 60 subsection 1 of the Copyright Act.

In ..... date ....

Author's signature

I dedicate this thesis to my family and friends, whose unwavering support and encouragement have been my constant source of strength throughout this journey. However, this work is mostly dedicated to my supervisor, doc. RNDr. Robert Švarc, Ph.D., whose guidance and expertise were invaluable. His patience, friendly approach, and the care he took in commenting and suggesting modifications were essential to the completion of this work.

Title: Continuous and distributional description of impulsive gravitational waves

Author: Matyáš Bílek

Institute: Institute of Theoretical Physics

Supervisor: doc. RNDr. Robert Švarc, Ph.D., Institute of theoretical physics

Abstract: This thesis explores the continuous and distributional descriptions of impulsive gravitational waves, focusing on nonexpanding and expanding waves propagating in Minkowski, de Sitter, and anti-de Sitter backgrounds. It employs cut-and-paste techniques and sandwich wave solutions to illustrate the construction of these models. Their influence on free test particles is examined. The research should highlight mathematical implications and delicacy related to the appearance of Dirac δ-distribution in curvature tensors and provide deeper insight into the shift and refraction of geodesics interacting with the expanding gravitational impulses. These findings should contribute to a better understanding of low-regularity space-times in general.

Keywords: low regularity spacetimes, impulsive gravitational waves, geodesics adapted coordinates

Název práce: Spojitý a distribuční popis impulzních gravitačních vln

Autor: Matyáš Bílek

Ústav: Ústav teoretické fyziky

Vedoucí práce: doc. RNDr. Robert Švarc, Ph.D., Ústav teoretické fyziky

Abstrakt: Tato práce se zabývá spojitým a distribučním popisem impulsních gravitačních vln, přičemž se zaměřuje na neexpandující a expandující vlny šířící se na Minkowského, de Sitterově a anti-de Sitterově pozadí. K ilustraci konstrukce těchto modelů používá techniku cut-and-paste a sendvičová vlnová řešení. Je zkoumán jejich vliv na volné testovací částice. Výzkum by měl zdůraznit matematické důsledky a jemnosti dané přítomností Diracovy δ distribuce v tenzorech křivosti a poskytnout hlubší vhled do posunu a ohybu geodetik interagujících s expandujícími gravitačními impulsy. Tyto poznatky by měly přispět k lepšímu pochopení prostoročasů nízké regularity na obecné úrovni.

Klíčová slova: prostoročasy s nízkou regularitou, impulsní gravitační vlny, geodetiky, adaptované souřadnice

Contents

Preface

General Relativity (GR) is a beautiful and bountiful theory of gravity. Since its formulation by Albert Einstein in 1915[1], it has helped resolve conundrums in many fields of physics, from particle physics to cosmology, the contribution of GR is indisputable. The point of merit is in using the theory of differential manifolds as the building stone for the description of the gravitational field [2, 3]. In the mathematical apparatus of differential geometry, spacetime is represented as a differentiable manifold $\mathcal{M}$ endowed with metric tensor $g_{\mu\nu}$. The gravitational field is identified with the structure of spacetime itself – its curvature – rather than being an added construct in spacetime to describe gravitational interaction.

Analogously to the way the electromagnetic field is related to the distribution of charges, and currents through Maxwell's equations, the gravitation law in the form of Einstein's field equations (EFE) relates the spacetime geometry to the distribution of mass-energy, momentum, and stress. This distribution provided via the stress-energy-momentum tensor $T_{\mu\nu}$ determines via EFE the metric tensor of the spacetime. In particular, the EFE is a set of ten nonlinear partial differential equations[1] for the metric tensor $g_{\mu\nu}$,

$$R_{\mu\nu} - \frac{1}{2}Rg_{\mu\nu} + \Lambda g_{\mu\nu} = \frac{8\pi G}{c^4}T_{\mu\nu}\,. \tag{1}$$

On the left-hand side of these equations, we have the Ricci tensor $R_{\mu\nu}$ obtained as a trace of the Riemann curvature tensor $R^{\mu}{}_{\nu\xi\rho}$. The scalar curvature R, which is obtained as a trace of the Ricci tensor, and a constant Λ representing the cosmological term.

Here, let us summarize the definitions of important geometrical objects and crucial concepts that are going to be useful in the rest of the thesis. First, we define the Riemann curvature tensor corresponding to the Levi-Civita connection[2] as follows

$$R^{\mu}{}_{\nu\xi\rho} \coloneqq \Gamma^{\mu}{}_{\nu\rho,\xi} - \Gamma^{\mu}{}_{\nu\xi,\rho} + \Gamma^{\mu}{}_{\kappa\xi}\Gamma^{\kappa}{}_{\nu\rho} - \Gamma^{\mu}{}_{\kappa\rho}\Gamma^{\kappa}{}_{\nu\xi}\,, \tag{2}$$

where $\Gamma^{\mu}{}_{\nu\xi}$ denotes the Christoffel symbols defined as

$$\Gamma^{\mu}{}_{\nu\xi} \coloneqq \frac{1}{2}g^{\mu\kappa}(g_{\kappa\nu,\xi} + g_{\kappa\xi,\nu} - g_{\nu\xi,\kappa})\,. \tag{3}$$

Employing the metric contraction, the Ricci tensor, and subsequently the scalar curvature is

$$R_{\mu\nu} \coloneqq R^{\kappa}{}_{\mu\kappa\nu}\,, \qquad R \coloneqq g^{\mu\nu}R_{\mu\nu}\,. \tag{4}$$

It is not surprising that finding any (exact) solution to EFE proves rather tricky [4], and understanding its physical consequences is typically not straightforward [5, 6]. For example, through apriori assumptions on spacetime symmetries, various exact solutions to EFE can be found although the resulting spacetimes are just an idealization of realistic situations, where the perturbative or numerical techniques have to be employed. Despite that, exact solutions are essential, as they provide us with tools for better comprehension of GR, and description of

[1] This is the only place, where we do not use the geometric units with $c = 1 = G$.

[2] That is metric and torsion-free covariant derivative.

gravity in general. Here, we have to at least mention extremely successful FLRW cosmological models [7, 8, 9], or geometry of the rotating Kerr black hole [10]. Nevertheless, the thesis is going to focus on another important GR prediction – gravitational waves. However, only in simple model situations represented by so-called impulsive gravitational waves, see [5] for a comprehensive review, and following chapters for the particular original references.

Returning to the geometrical concepts, in the thesis we will analyze trajectories of free test particles, and how they are affected by the gravitational impulse. In terms of differential geometry, the trajectories of free test particles are geodesics. We can thus obtain these trajectories by solving the geodesic equation. We call a curve $z^\mu(\alpha) : \mathbb{R} \mapsto \mathcal{M}$ a geodetic parameterized by affine parameter α, if it satisfy the geodesic equation

$$\frac{\mathrm{d}^2 z^\mu}{\mathrm{d}\alpha^2} + \Gamma^\mu{}_{\nu\xi} \frac{\mathrm{d}z^\nu}{\mathrm{d}\alpha} \frac{\mathrm{d}z^\xi}{\mathrm{d}\alpha} = 0\,. \tag{5}$$

To characterize spacetime – its free gravitational field – we want to further introduce the Weyl tensor as a traceless component of the Riemann tensor, namely

$$C_{\mu\nu\xi\kappa} = R_{\mu\nu\xi\kappa} - \frac{4}{D-2} R_{[\mu|[\xi} g_{\kappa]|\nu]} + \frac{2}{(D-1)(D-2)} R g_{[\mu|[\xi} g_{\kappa]|\nu]}\,, \tag{6}$$

where D stands for the spacetime dimension[3].

Since the curvature contribution in EFE is represented only by the traces of the Riemann tensor, some components are not determined directly by the gravitational law. Essentially, these components are encoded in the Weyl tensor, which can be non-trivial even in the empty vacuum spacetime. The Weyl tensor can be understood as representing "free components" of the gravitational field, see e.g. [4, 5][4].

As mentioned earlier we are going to be considering particular exact solutions called impulsive gravitational waves within the thesis. Formally, these are exact spacetimes solving EFE whose metric tensor is at least C^3 almost everywhere, but for a specific hypersurface $\mathcal{N}$ where it is only of regularity C^0. In general, this results in some components of the curvature containing Dirac δ-distribution. If the hypersurface $\mathcal{N}$ is *null*, then we can interpret these spacetimes as impulsive waves. Moreover, if the δ-distribution is in the Weyl tensor, we deal with the impulsive gravitational waves. On the contrary, we can also have the distributional impulsive components in the Ricci tensor, thus representing some kind of matter with a distributional profile.

Geometrically and algebraically speaking, we are going to be working with impulsive limits of solutions either of the Kundt type N spacetimes or the Robinson–Trautman type N spacetimes, respectively. Detailed classification and geometrical consequences can be found in [5, 11]. In both cases, the waves propagate on the backgrounds of spacetimes of constant curvature, i.e., either Minkowski, de Sitter, or anti-de Sitter spacetime, everywhere but on the hypersurface $\mathcal{N}$. Expanding Robinson-Trautman and non-expanding Kundt impulsive solutions in

[3] All the above expressions work in arbitrary dimension D, however, we will be interested in the classic case $D = 4$.

[4] Interestingly, in $D = 3$ there is no free component of the gravitational field and complete geometry is determined by the EFE.

the constant curvature backgrounds are distinct by the null hypersurface geometry which is naturally reflected by the action of the impulse. In general, these two important and large solution classes containing not only type N wave-like solutions are identified in terms of the admitted null congruence of geodesics and its behavior. In both cases, there exists non-shearing and non-twisting null geodesic congruence which is additionally *nonexpanding* in the Kundt class, while it *expands* in the Robinson–Trautman one, see also [5] for a comprehensive review.

As a review, our main goal is to provide a detailed description of continuous and distributional forms of impulsive gravitational waves propagating in constant curvature backgrounds. We summarize a construction of these exact solutions to Einstein's field equations, and analyze their effects on geodesics. By focusing on nonexpanding and expanding impulsive waves in Minkowski, we seek to understand the mathematical implications of Dirac δ-distributions in curvature tensors, the suitability of coordinate parameterization, and the influence on geodesic behavior.

The thesis is organized as follows. In chapter 1, we describe the basic characteristics of the constant curvature backgrounds, that is Minkowski, de Sitter, and Anti-de Sitter spacetimes. Chapter 2 focuses on the construction of impulsive gravitational waves, detailing methods such as the cut-and-paste technique, and the limits of sandwich wave solutions. Chapter 3 shows how to examine the geodesics in impulsive gravitational waves, and explores the behavior of nonexpanding and expanding waves, and their description in terms of the continuous coordinates. Finally, chapter 4 discusses the geodesics in the expanding spacetime with a snapped cosmic string. The implications of refraction formulae both for general geodesics, and the privileged ones are visualized. The thesis concludes with a summary of our findings, and their possible implications and extensions.

1. spacetime of constant curvature

In this chapter, we describe the basic characteristics of spacetimes, that will serve as backgrounds for the propagation of impulsive gravitational waves, we will guide ourselves by [5].

These spacetimes can be introduced as maximally symmetric vacuum solutions of Einstein's field equations (2). A four-dimensional spacetime has a maximum of 10 symmetries. These isometries correspond to four translations, three spatial rotations, and three Lorentz boosts. The maximal number of symmetries constrain the curvature of such spacetime. In particular, it has to be *constant*. This allows us to express the Riemann tensor in the form

$$R_{\mu\nu\xi\kappa} = \frac{1}{12} R \left(g_{\mu\xi} g_{\nu\kappa} - g_{\mu\kappa} g_{\nu\xi} \right),$$

where the constant scalar curvature R is given via contraction of EFE (2) by the cosmological term Λ as $R = 4\Lambda$.

Corresponding to the sign of R we may distinguish three qualitatively different types of constant curvature spacetimes. In particular, if R vanishes we have Minkowski spacetime, for $R > 0$ we have de Sitter spacetime, and for $R < 0$ we have anti-de Sitter spacetime. In other words, we see that Minkowski, de Sitter, and anti-de Sitter spacetimes are maximally symmetric vacuum solutions of field equations with vanishing, positive, and negative cosmological constant Λ, respectively. Furthermore, it can be shown that these three spacetimes are the vacuum solutions of (2) with vanishing Weyl tensor $C_{\mu\nu\xi\kappa} = 0$.

1.1 Minkowski spacetime

Minkowski spacetime is the simplest solution of the Einstein field equations. It has vanishing curvature, i.e., it is flat at every point, and does not contain any matter or gravitational field. In terms of the Riemann tensor, the Minkowski spacetime can always be identified through the condition $R_{\mu\nu\xi\kappa} = 0$. It is used as the spacetime geometry in special relativity, where the metric of Minkowski spacetime is typically denoted as $\eta_{\mu\nu}$, but we will not use such a notation.

1.1.1 Coordinate representation

The metric in standard Cartesian coordinates is

$$\mathrm{d}s^2 = -\mathrm{d}t^2 + \mathrm{d}x^2 + \mathrm{d}y^2 + \mathrm{d}z^2 , \tag{1.1}$$

where the range of all coordinates is $\mathbb{R}$. We can transform the metric to other coordinates representing the same spacetime. However, we may find that such a procedure introduces some nonphysical features such as coordinate singularities. For example, a transformation to spherical coordinates gives us

$$\mathrm{d}s^2 = -\mathrm{d}t^2 + \mathrm{d}r^2 + r^2 \left(\mathrm{d}\theta^2 + \sin^2\theta \, \mathrm{d}\phi^2 \right), \tag{1.2}$$

where the metric has apparent singularities for $r = 0$, $\sin(\theta) = 0$ or as $r \to \infty$. There is no physical meaning in these apparent (coordinate) singularities; however, it is tricky to identify their nature within more involved cases than a flat space.

For purposes of impulsive wave description, we introduce the double *null coordinates*. They are related to the Cartesian coordinates as

$$u = \frac{1}{\sqrt{2}}(t - z)\,, \qquad v = \frac{1}{\sqrt{2}}(t + z)\,,$$

the line element (1.1) becomes now of the form

$$\mathrm{d}s^2 = -2\mathrm{d}u\mathrm{d}v + \mathrm{d}x^2 + \mathrm{d}y^2\,. \tag{1.3}$$

These coordinates foliate the spacetime by a family of *null planes* perpendicular to xy-plane, and given by conditions $u = \text{const}$ and $v = \text{const}$, respectively, see figure 2.1 in the case of nonexpanding impulses. Furthermore, we can cover the xy-plane by a single *complex* coordinate, i.e., transform the metric using

$$\zeta = \frac{1}{\sqrt{2}}(x + iy)\,.$$

Immediately, we get

$$\mathrm{d}s^2 = -2\mathrm{d}u\mathrm{d}v + 2\mathrm{d}\zeta\mathrm{d}\bar{\zeta}\,. \tag{1.4}$$

If we start with Minkowski space (1.2) in spherical coordinates, we can perform an alternative transformation to *null coordinates*, namely

$$\mathrm{U} = \frac{1}{\sqrt{2}}(t - r)\,, \qquad \mathrm{V} = \frac{1}{\sqrt{2}}(t + r)\,,$$

which leads to the line element

$$\mathrm{d}s^2 = -2\mathrm{d}\mathrm{U}\mathrm{d}\mathrm{V} + \frac{1}{2}(\mathrm{U}^2 - \mathrm{V}^2)\left(\mathrm{d}\theta^2 + \sin^2\theta\,\mathrm{d}\phi^2\right). \tag{1.5}$$

In this case, we foliate the spacetime by two families of *null cones* for U and V equal to constant, respectively. Here, each point of such a hypersurface represents a 2-sphere with radius $r = \frac{1}{\sqrt{2}}|\mathrm{U} - \mathrm{V}|$. In other words, for U and V constant, we are left with hypersurfaces of positive Gaussian curvature. Finally, we can directly transform the metric (1.4) to this form using

$$\begin{aligned} u &= \frac{1}{2}\left[\mathrm{U}(1 - \cos\theta) + \mathrm{V}(1 + \cos\theta)\right], \\ v &= \frac{1}{2}\left[\mathrm{U}(1 + \cos\theta) + \mathrm{V}(1 - \cos\theta)\right], \\ \zeta &= \frac{1}{2}(\mathrm{U} - \mathrm{V})\sin\theta\exp i\phi\,. \end{aligned}$$

Moreover, there also exists a different transformation of coordinates that gives the *single null cone* foliation of Minkowski spacetime, see figure 2.2 for the case of expanding impulses. The resulting metric will be important for our further discussion of expanding impulses. Within this parameterization, one has an additional parameter ϵ that is related to the Gaussian curvature of the 2-surface

given by constant U coordinate. To be explicit, we start from (1.4) with the transformation

$$\begin{aligned} u &= \frac{Z\bar{Z}}{p}\mathrm{V} - \mathrm{U}\,, \\ v &= \frac{\mathrm{V}}{p} - \epsilon\mathrm{U}\,, \\ \zeta &= \frac{\mathrm{Z}}{p}\mathrm{V}\,, \end{aligned}$$

where

$$p = 1 + \epsilon Z\bar{Z}\,, \qquad \epsilon = -1, 0, 1\,.$$

This transformation gives us the Minkowski metric in the form

$$\mathrm{d}s^2 = 2\frac{\mathrm{V}^2}{p^2}\mathrm{d}Z\mathrm{d}\bar{Z} + 2\mathrm{d}\mathrm{U}\mathrm{d}\mathrm{V} - \epsilon\mathrm{d}\mathrm{U}^2\,. \tag{1.6}$$

A detailed description of these coordinates and spacetime foliation can be found e.g. in [5]. In particular, in these coordinates the hypersurface given by U equal to constant is a *future null cone*, since $\mathrm{U}(\mathrm{V} - \epsilon\mathrm{U}) = \zeta\bar{\zeta} - uv = 0$. By inverting the coordinate transformation for $\epsilon \neq 0$ we get

$$\mathrm{U} = \frac{2\zeta\bar{\zeta}}{-(v-\epsilon u) \pm \sqrt{(v-\epsilon u)^2 + 4\epsilon\zeta\bar{\zeta}}} - \epsilon v\,,$$

$$\mathrm{V} = \frac{4\epsilon\zeta\bar{\zeta}}{-(v-\epsilon u) \pm \sqrt{(v-\epsilon u)^2 + 4\epsilon\zeta\bar{\zeta}}} - (v-\epsilon u)\,,$$

$$Z = \frac{\epsilon}{2\bar{\zeta}}\big(-(v-\epsilon u) \pm \sqrt{(v-\epsilon u)^2 + 4\epsilon\zeta\bar{\zeta}}\big)\,.$$

We can find a rather simple relations between (1.5) and (1.6) for $\epsilon = +1$ and positive and negative branch of Z respectively

$$\begin{aligned} \mathrm{U}_+ &= -\mathrm{u} = \frac{1}{\sqrt{2}}(r-t)\,, & \mathrm{U}_- &= -\mathrm{v} = -\frac{1}{\sqrt{2}}(t+r)\,, \\ \mathrm{V}_+ &= \mathrm{v} - \mathrm{u} = \sqrt{2}r\,, & \mathrm{V}_- &= \mathrm{u} - \mathrm{v} = -\sqrt{2}r\,, \\ Z_+ &= -\frac{\sin\theta}{1+\cos\theta}\exp i\phi = \frac{x-iy}{r+z}\,, & Z_- &= \frac{\sin\theta}{1-\cos\theta}\exp i\phi = \frac{x+iy}{r-z}\,. \end{aligned}$$

From this transformation, we see that in (1.6) the coordinate V is equivalent to the radius, and that $Z, \bar{Z}$ are coordinates of stereographic projection of a sphere of radius r from north pole for Z_- and from south pole for Z_+, respectively. We may also find equivalent relation between (1.1) or (1.5) and (1.6) for $\epsilon = -1$. For $\epsilon = 0$ we can find the relation between (1.1) and (1.6) in [5] on page 403.

1.1.2 A model for cosmic string

Motivated by the expanding impulsive gravitational waves, see chapter 4, we introduce a topological defect into the flat space, which represents the so-called cosmic string. To do so, we can also describe Minkowski spacetime via cylindrical coordinates. From (1.1) we use the classical transformation to get

$$\mathrm{d}s^2 = -\mathrm{d}t^2 + \mathrm{d}\rho^2 + \rho^2\mathrm{d}\phi^2 + \mathrm{d}z^2\,, \tag{1.7}$$

where $\rho \in [0, \infty)$ and $\phi \in [0, 2\pi)$. There is a coordinate singularity at the axis $\rho = 0$, but we know that it is just an apparent one.

Now, we artificially remove a wedge of angle $2\pi\delta$ in all spatial sections around the z axis simply by taking $\phi \in [0, (1-\delta)2\pi)$. We must identify the two edges of the missing wedge to have a continuous spacetime. The resulting spacetime remains flat everywhere, except for the axis $\rho = 0$. We can illustrate this spacetime by taking t and z constant, the resulting surface is the surface of a cone.

Then, in contrast with (1.7) we have a spacetime whose curvature tensor vanishes everywhere except the axis. We have to conclude that the axis is singular in itself, i.e., it is not just an apparent singularity due to our choice of coordinates. In this simple way, we constructed a topological defect in our spacetime, which is often referred to as *conical singularity*.

Moreover, we would like to write down the line element for this spacetime. It is more convenient to introduce rescaled variable φ as $\varphi = (1-\delta)\phi$ where $\phi \in [0, 2\pi)$. We further denote $(1-\delta)$ as C. We get

$$\mathrm{d}s^2 = -\mathrm{d}t^2 + \mathrm{d}\rho^2 + C^2\rho^2\mathrm{d}\varphi^2 + \mathrm{d}z^2\,. \tag{1.8}$$

It can be shown that a pair of parallel lines approaching the axis $\rho = 0$ from either side will start to converge after passing the axis. Despite that spacetime is locally flat everywhere, except along the axis, i.e., no tidal gravitational forces occur, the conical singularity still has a global focusing effect on geodesics passing it from either side. This is similar to having a gravitational source in the spacetime; however, the curvature does not diverge at the singularity.

The Ricci tensor contains a distributional component along the z-axis, through EFE this contribution corresponds to a non-zero stress component in the energy-momentum tensor. Thus we can identify this spacetime with one that incorporates an infinite line source under constant tension.

This describes a simple model of the *cosmic string*. The deficit angle is proportional to the mass per unit length of the string μ given by $\mu = \frac{1}{4}\delta = \frac{1}{4}(1-C)$. Finally, we must stress out that this is not the usual kind of gravitational mass as the the surrounding field is locally flat. We want to mention that it is also possible to get a string under constant compression having $\mu < 0$, this corresponds to an excessive angle $\delta < 0$.

1.2 (Anti-)de Sitter spacetime

As mentioned at the beginning of this chapter, (anti-)de Sitter spacetimes (shortly AdS and dS) are maximally symmetric vacuum solutions of EFE with positive cosmological constant Λ for dS and negative Λ for AdS. Their scalar curvature is

given by $R = 4\Lambda$. Both de Sitter and anti-de Sitter manifolds can be visualized geometrically as hyperboloids

$$-Z_0^2 + Z_1^2 + Z_2^2 + Z_3^2 \pm Z_4^2 = \pm a^2\,, \qquad a = \sqrt{\frac{3}{|\Lambda|}}\,, \tag{1.9}$$

embedded in a five-dimensional flat space

$$\mathrm{d}s^2 = -\mathrm{d}Z_0^2 + \mathrm{d}Z_1^2 + \mathrm{d}Z_2^2 + \mathrm{d}Z_3^2 \pm \mathrm{d}Z_4^2\,, \tag{1.10}$$

where we have + for dS and − for AdS, respectively.

Symmetries of the de Sitter spacetime are characterized by the ten-parameter group $SO(1,4)$. For the anti-de Sitter spacetime, we recognize that it has two timelike dimensions Z_0 and Z_4. This representation of AdS space is related to its symmetry structure characterized by the ten-parameter group $SO(2,3)$. We can transform the metric (1.10) by using the parameterization

$$\begin{aligned}
Z_0 &= \frac{1}{\sqrt{2}}(v+u)\left[1 - \tfrac{1}{6}\Lambda(uv - \zeta\bar{\zeta})\right]^{-1}\,,\\
Z_1 &= \frac{1}{\sqrt{2}}(v-u)[1 - \frac{1}{6}\Lambda(uv - \zeta\bar{\zeta})]^{-1}\,,\\
Z_2 &= \frac{1}{\sqrt{2}}(\zeta+\bar{\zeta})[1 - \frac{1}{6}\Lambda(uv - \zeta\bar{\zeta})]^{-1}\,,\\
Z_3 &= \frac{1}{\sqrt{2}}(\zeta-\bar{\zeta})[1 - \frac{1}{6}\Lambda(uv - \zeta\bar{\zeta})]^{-1}\,,\\
Z_4 &= a[1 + \frac{1}{6}\Lambda(uv - \zeta\bar{\zeta})][1 - \frac{1}{6}\Lambda(uv - \zeta\bar{\zeta})]^{-1}\,,
\end{aligned}$$

with $u, v \in (-\infty, +\infty)$, and $\zeta \in \mathbb{C}$. This parameterization covers globally the whole dS and AdS hyperboloids, except for the coordinate singularities at $u, v = \infty$, and gives the manifestly conformally flat line element

$$\mathrm{d}s^2 = \frac{-2\mathrm{d}u\mathrm{d}v + 2\mathrm{d}\zeta\mathrm{d}\bar{\zeta}}{[1 - \frac{1}{6}\Lambda(uv - \zeta\bar{\zeta})]^2}\,. \tag{1.11}$$

This line element gives us an unified form for either Minkowski, de Sitter, or anti-de Sitter spacetime depending on the sign of cosmological constant Λ. For clarity, we add the inverse transformation, namely

$$u = \sqrt{2}a\frac{Z_0 - Z_1}{Z_4 + a}\,, \qquad v = \sqrt{2}a\frac{Z_0 + Z_1}{Z_4 + a}\,, \qquad \zeta = \sqrt{2}a\frac{Z_2 + iZ_3}{Z_4 + a}\,.$$

2. Impulsive waves and their construction

Here, we are going to briefly describe how to obtain spacetime with impulsive gravitational waves.Wwe will use spacetimes with constant curvature as our backgrounds. In these backgrounds, such waves belong to two distinct solution families, Kundt type N spacetimes and Robinson–Trautman type N spacetimes [5, 11]. The difference corresponds to properties of the null congruences perpendicular to the impulse. It is non-twisting, shear-free, and has zero or non-zero expansion, respectively. Starting from the constant curvature backgrounds, there are various methods of particular solution constructions, both for nonexpanding and expanding cases.

The history of studies of impulsive waves can be divided into three periods as stated in [11]. During the first one, principal mathematical properties of shock waves in GR were investigated, culminating with the works of Lichnerowicz and Synge. It was shown that these waves must be located on null hypersurfaces across which the metric derivatives must be discontinuous.

The second era could be called the "Golden Age" of gravitational impulses. Here, the first explicit methods of construction leading to impulsive solutions were found in the works of Penrose [12] and Aichelburg and Sexl [13]. Most of these methods were subsequently discovered in the 1970s.

The last era starts at the beginning of the 1990s with the paper by Hotta and Tanaka. They constructed nonexpanding impulse in the de Sitter and anti-de sitter spacetimes in analogy with Aichelburg and Sexl. They boosted the Schwarzschild black hole in these spacetimes to the speed of light. Furthermore, an expanding impulsive wave solution created by the snapping of cosmic string in Minkowski spacetime was discovered and discussed by Gleiser and Pulin, Bičák, Hogan, Nutku and Penrose, Podolský and Griffiths and others [14, 11, 15, 16, 17].

2.1 Cut and paste construction

A geometrical method for the construction of nonexpanding and expanding impulsive waves in Minkowski background was introduced by Roger Penrose [12]. This method was later extended for de Sitter and anti-de Sitter spacetimes. In general, this method is based on cutting the background spacetime manifold $\mathcal{M}$ along a suitable null hypersurface $\mathcal{N}$, and re-attaching it back with a warp meeting the Penrose junction conditions.

2.1.1 Nonexpanding impulsive waves

In this case, the method is based on removing a plane from our background space. The hypersurface $\mathcal{N}$ is a null plane identified as the hypersurface $u = 0$ in the null coordinates

$$\mathrm{d}s^2 = \frac{-2\mathrm{d}u\mathrm{d}v + 2\mathrm{d}\zeta\mathrm{d}\bar{\zeta}}{[1 - \frac{1}{6}\Lambda(uv - \zeta\bar{\zeta})]^2}\,. \tag{2.1}$$

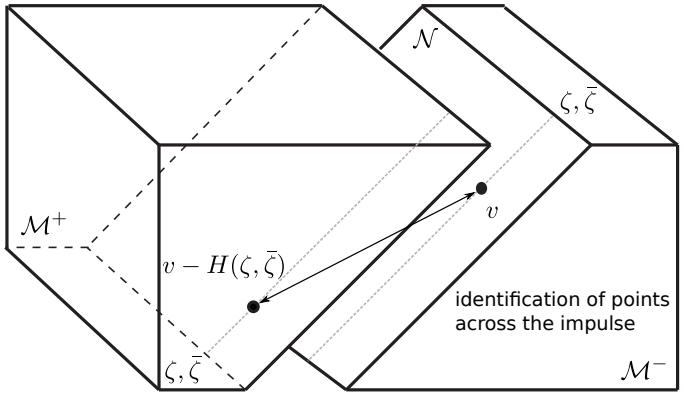

Figure 2.1: Schematic illustration of the Penrose cut and paste construction in the case of nonexpanding impulses.

Now, we just re-attach the two space $\mathcal{M}_-$ with $u < 0$ and $\mathcal{M}_+$ defined by $u > 0$ in a way such that they satisfy the Penrose warp condition

$$\left[\zeta, \bar{\zeta}, v, u = 0_-\right]_{\mathcal{M}_-} \equiv \left[\zeta, \bar{\zeta}, v - H(\zeta, \bar{\zeta}), u = 0_+\right]_{\mathcal{M}_+} , \tag{2.2}$$

where H is an arbitrary function of spatial complex variables, see figure 2.1.

Penrose showed that satisfying these conditions implies that the metric solves the EFE everywhere, even on the hypersurface $u = 0$ with the constraint on $H_{,\zeta\bar{\zeta}}$ [12]. In particular, the condition can be expressed as

$$H(\zeta, \bar{\zeta}) = f(\zeta) + g(\bar{\zeta}) . \tag{2.3}$$

For the curvature tensor, impulsive components proportional to $\delta(u)$ are obtained in a suitable frame. This approach introduces nonexpanding impulsive gravitational waves in Minkowski, de Sitter, and anti-de Sitter spaces, where the difference between these three cases can be seen in the character of the 2-surface spanned by coordinates $\zeta, \bar{\zeta}$. It is a space of constant Gaussian curvature $K = \frac{\Lambda}{3}$. Thus for $\Lambda = 0$, it is a plane and we obtain the so-called *pp-waves*, i.e., plane-fronted waves with parallel propagation. Furthermore, when Λ is positive, spherical waves occur, whereas for negative Λ, the wave surface is a hyperboloid.

2.1.2 Expanding impulsive waves

In the same manner, we remove a hypersurface $\mathcal{N}$ however it should create a null cone this time. To do so, we use the suitable parametrization (1.6)

$$\mathrm{d}s^2 = \frac{2(\mathrm{V}^2/p^2)\mathrm{d}Z\mathrm{d}\bar{Z} + 2\mathrm{d}\mathrm{U}\mathrm{d}\mathrm{V} - \epsilon\mathrm{d}\mathrm{U}^2}{[1 + \frac{1}{6}\Lambda\mathrm{U}(\mathrm{V} - \epsilon\mathrm{U})]^2} . \tag{2.4}$$

In these coordinates, $\mathrm{U} = 0$ is a future *null cone* with the geometry of an expanding sphere. Analogously to the non-expanding case, we divide the spacetime into two pieces, the inner part of null cone $\mathcal{M}_-$ with $\mathrm{U} < 0$, and its outer part $\mathcal{M}_+$ with $\mathrm{U} > 0$. Now, we reattach these parts back together with a warp generated

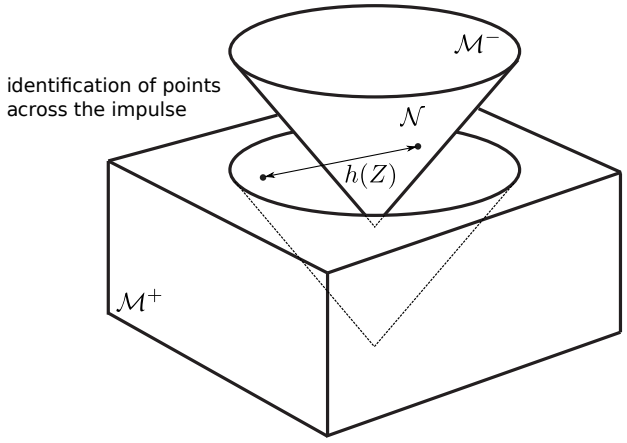

Figure 2.2: Schematic illustration of the Penrose cut and paste construction in the case of expanding impulses.

by an arbitrary complex-valued function $h(Z)$. The Penrose junction conditions prescribe the identification across $\mathcal{N}$ as

$$\left[Z,\, \bar{Z},\, \mathrm{V},\, \mathrm{U}=0_-\right]_{\mathcal{M}_-} \equiv \left[h(Z),\, h(\bar{Z}),\, \frac{1+\epsilon h\bar{h}}{1+\epsilon Z\bar{Z}}\frac{\mathrm{V}}{|h'|},\, \mathrm{U}=0_+\right]_{\mathcal{M}_+}, \qquad (2.5)$$

see figure 2.2 showing such a construction.

2.2 Continuous coordinates

The cut-and-paste construction method is general. By prescribing the junction conditions, we can construct all nonexpanding and expanding impulsive gravitational waves in Minkowski, de Sitter, and anti-de Sitter spacetimes. Despite that, it is a formal method of identifying points on both sides of the impulse, and does not yield explicit metric forms of the complete spacetime. However, it is of utter interest for us to express such spaces in the coordinate system where the metric is explicitly continuous everywhere, even across the impulse. Here, we list these privileged coordinate systems for non-expanding and expanding impulses. However, we will describe their construction later. In the next sections, we will closely follow [18] for nonexpanding impulsive waves, and [19] for expanding impulses.

2.2.1 Nonexpanding impulsive waves

We will start again with the metric (1.11). Now we perform the transformation

$$u = U\,, \qquad v = V + H + UH_{,Z}H_{,\bar{Z}}\,, \qquad \zeta = Z + UH_{,\bar{Z}}\,,$$

where $H(Z,\bar{Z})$ is an arbitrary real function. This results in the metric

$$\mathrm{d}s_0^2 = \frac{2|\mathrm{d}Z + U(H_{,Z\bar{Z}}\mathrm{d}Z + H_{,\bar{Z}\bar{Z}}\mathrm{d}\bar{Z})|^2 - 2\mathrm{d}U\mathrm{d}V}{[1+\frac{1}{6}\Lambda(Z\bar{Z}-UV-UG)]^2}\,, \qquad (2.6)$$

where

$$G = H - ZH_{,Z} - \bar{Z}H_{,\bar{Z}}\,.$$

Now, we consider this metric for $U > 0$, and combine it with (1.11) for $U < 0$ in which we just re-label coordinates as

$$u = U\,, \qquad v = V\,, \qquad \zeta = Z\,.$$

In other words, we take (1.11) in front of the impulse, and (2.6) behind the impulse. The resulting global metric can be written as

$$\mathrm{d}s^2 = \frac{2|\mathrm{d}Z + U\Theta(U)(H_{,Z\bar{Z}}\mathrm{d}Z + H_{,\bar{Z}\bar{Z}}\mathrm{d}\bar{Z})|^2 - 2\mathrm{d}U\mathrm{d}V}{[1 + \frac{1}{6}\Lambda(Z\bar{Z} - UV - U\Theta(U)G)]^2}\,, \tag{2.7}$$

where $\Theta(U)$ is the *Heaviside step function*. This metric is continuous across the impulse at $U = 0$; however, there are discontinuities in the derives of the metric. Components of the Weyl tensor and curvature tensors are proportional to the *Dirac distribution*. This metric is an explicit realization of the Penrose junction conditions.

This line element thus explicitly describes nonexpanding impulsive waves in constant curvature spacetimes. For $\Lambda = 0$ it reduces to the well-known Rosen form of impulsive *pp*-waves. The transformation relating the continuous metric (2.7) and explicitly impulsive Brinkmann form,

$$\mathrm{d}s^2 = \frac{2\,\mathrm{d}\zeta\,\mathrm{d}\bar{\zeta} - 2\,\mathrm{d}u\,\mathrm{d}v + 2H(\zeta,\bar{\zeta})\,\delta(u)\,\mathrm{d}u^2}{[\,1 + \frac{1}{6}\Lambda(\zeta\bar{\zeta} - uv)\,]^2}\,, \tag{2.8}$$

can be written as

$$\begin{aligned} u &= U\,, \\ v &= V + H\Theta(U) + U\Theta(U)H_{,Z}H_{,\bar{Z}}\,, \\ \zeta &= Z + U\Theta(U)H_{,\bar{Z}}\,. \end{aligned} \tag{2.9}$$

We can see that it is discontinuous in the v coordinate for $u = 0$. This transformation allows us to easily obtain the Penrose junction conditions for nonexpanding impulses (2.2) by its evaluation approaching $u = 0$ from above and below.

The discontinuity causes some mathematical problems; however, it was shown that it is possible to interpret this transformation as a distributional limit of smooth transformations obtained by a generic regularisation procedure [20, 19].

2.2.2 Expanding impulsive waves

In the expanding case, we need to perform a much more complex transformation of the metric (1.11) to explicitly construct spacetime that satisfies the Penrose junction conditions [21]. We start with

$$\begin{aligned} v &= A\mathrm{V} - D\mathrm{U}\,, \\ u &= B\mathrm{V} - E\mathrm{U}\,, \\ \zeta &= C\mathrm{V} - F\mathrm{U}\,, \end{aligned} \tag{2.10}$$

where

$$
\begin{aligned}
A &= \frac{1}{p|h'|}, \qquad B = \frac{|h|^2}{p|h'|}, \qquad C = \frac{h}{p|h'|}\,, \\
D &= \frac{1}{|h'|}\left[\frac{p}{4}\left|\frac{h''}{h'}\right|^2 + \epsilon\left(1 + \frac{Z}{2}\frac{h''}{h'} + \frac{\bar{Z}}{2}\frac{\bar{h}''}{\bar{h}'}\right)\right], \\
E &= \frac{|h|^2}{|h'|}\left[\frac{p}{4}\left|\frac{h''}{h'} - 2\frac{h'}{h}\right|^2 + \epsilon\left(1 + \frac{Z}{2}\left(\frac{h''}{h'} - 2\frac{h'}{h}\right) + \frac{\bar{Z}}{2}\left(\frac{\bar{h}''}{\bar{h}'} - 2\frac{\bar{h}'}{\bar{h}}\right)\right)\right], \\
F &= \frac{h}{|h'|}\left[\frac{p}{4}\left(\frac{h''}{h'} - 2\frac{h'}{h}\right)\frac{\bar{h}''}{\bar{h}'} + \epsilon\left(1 + \frac{Z}{2}\left(\frac{h''}{h'} - 2\frac{h'}{h}\right) + \frac{\bar{Z}}{2}\frac{\bar{h}''}{\bar{h}'}\right)\right],
\end{aligned}
\tag{2.11}
$$

and h remains consistent with the junction conditions(2.5). This transformation is generalizing the null cone transformation (1.6). In both cases, the null cone $\mathcal{N}$ is located at $\mathrm{U} = 0$. This can be seen from the fact that the coefficients (2.11) and their derivatives satisfy the identities

$$
\begin{aligned}
AB - C\bar{C} &= 0, \\
DE - F\bar{F} &= \epsilon, \\
AE + BD - C\bar{F} - \bar{C}F &= 1, \\
DE_{,Z} + D_{,Z}E - F\bar{F}_{,Z} - F_{,Z}\bar{F} &= 0, \\
A_{,Z}E + B_{,Z}D - C_{,Z}\bar{F} - \bar{C}_{,Z}F &= 0, \\
A\,E_{,Z} + BD_{,Z} - C\bar{F}_{,Z} - \bar{C}F_{,Z} &= 0, \\
A_{,Z}B + AB_{,Z} - C_{,Z}\bar{C} - C\bar{C}_{,Z} &= 0, \\
A_{,Z}B_{,Z} - C_{,Z}\bar{C}_{,Z} &= 0, \\
D_{,Z}E_{,Z} - F_{,Z}\bar{F}_{,Z} &= 0, \\
A_{,Z}E_{,Z} + B_{,Z}D_{,Z} - C_{,Z}\bar{F}_{,Z} - \bar{C}_{,Z}F_{,Z} &= H, \\
C_{,Z}\bar{C}_{,\bar{Z}} + C_{,\bar{Z}}\bar{C}_{,Z} - A_{,Z}B_{,\bar{Z}} - A_{,\bar{Z}}B_{,Z} &= \frac{1}{p^2}, \\
F_{,Z}\bar{F}_{,\bar{Z}} + F_{,\bar{Z}}\bar{F}_{,Z} - D_{,Z}E_{,\bar{Z}} - D_{,\bar{Z}}E_{,Z} &= p^2|H|^2, \\
A_{,Z}E_{,\bar{Z}} + A_{,\bar{Z}}E_{,Z} + B_{,Z}D_{,\bar{Z}} + B_{,\bar{Z}}D_{,Z} & \\
-C_{,Z}\bar{F}_{,\bar{Z}} - C_{,\bar{Z}}\bar{F}_{,Z} - \bar{C}_{,Z}F_{,\bar{Z}} - \bar{C}_{,\bar{Z}}F_{,Z} &= 0\,,
\end{aligned}
\tag{2.12}
$$

together with their complex conjugates. This allows us to show that $\zeta\bar{\zeta} - uv = \mathrm{U}(\mathrm{V} - \epsilon\mathrm{U})$. Using the transformation (2.10), the metric becomes

$$
\mathrm{d}s^2 = \frac{2\left|\frac{\mathrm{V}}{p}\,\mathrm{d}Z + \mathrm{U}p\bar{H}\mathrm{d}\bar{Z}\right|^2 + 2\mathrm{d}\mathrm{U}\mathrm{V} - 2\epsilon\mathrm{d}\mathrm{U}^2}{\left[1 + \frac{1}{6}\Lambda\mathrm{U}\left(\mathrm{V} - \epsilon\mathrm{U}\right)\right]^2}\,, \tag{2.13}
$$

with

$$
H(Z) = \frac{1}{2}\left[\frac{h'''}{h'} - \frac{3}{2}\left(\frac{h''}{h'}\right)^2\right].
$$

For the trivial choice of the warp function $h(Z)$, i.e., for $h(Z) = Z$, we see that this reduces to the metric (1.6) where Z is the coordinate of stereographic

projection. As in the nonexpanding case, we combine these line elements across $\mathrm{U}=0$ introducing a *kink function*, namely $\mathrm{U}_+ = \mathrm{U}\Theta(\mathrm{U})$ in the metric by having (1.6) for $\mathrm{U}<0$, and (2.13) for $\mathrm{U}>0$. We obtain

$$\mathrm{d}s^2 = \frac{2\left|\frac{\mathrm{V}}{p}\,\mathrm{d}Z + \mathrm{U}_+ p\bar{H}\mathrm{d}\bar{Z}\right|^2 + 2\mathrm{dUV} - 2\epsilon\mathrm{dU}^2}{\left[1+\frac{1}{6}\Lambda\mathrm{U}\left(\mathrm{V}-\epsilon\mathrm{U}\right)\right]^2}\,. \tag{2.14}$$

Since the kink function is Lipschitz continuous, the metric is locally Lipschitz in U over the impulse. However, locally Lipschitz metric possesses no bound on the curvature, the discontinuity in the derivatives results in impulsive components in the Weyl and curvature tensors, namely $\Psi_4 = (p^2H/\mathrm{V})\delta(\mathrm{U})$, and $\Phi_{22} = (p^4H\bar{H}/\mathrm{V}^2)\mathrm{U}\delta(\mathrm{U})$. The spacetime is conformally flat everywhere, but for the impulsive surface $\mathrm{U}=0$. Moreover, there is a problem in the point $\mathrm{V},\mathrm{U}=0$ (origin of the impulse), and at possible poles of the function p^2H, as a curvature singularity is located there [19].

2.3 Limits of sandwich wave solutions

As was mentioned before, impulsive waves can be understood as distributional limits of sandwich waves in suitable families of radiative spacetimes. It is a very intuitive approach; however, there are various mathematical difficulties. Detailed understanding, especially in the case of expanding Robinson–Trautman impulses, is still an open problem.

2.3.1 Nonexpanding impulsive waves

We proceed from *pp*-waves for nonexpanding impulses. In this case, one obtains the metric

$$\mathrm{d}s^2 = 2\mathrm{d}\zeta\mathrm{d}\bar{\zeta} - 2\mathrm{d}u\mathrm{d}v + H(\zeta,\bar{\zeta})\delta(u)\mathrm{d}u^2\,. \tag{2.15}$$

This is the Brinkmann form of impulsive *pp*-waves on Minkowski background. Its generalizations for $\Lambda\neq 0$ are obtained similarly within the Kundt class of solutions. In general, it can be demonstrated that all nonexpanding impulses in constant curvature backgrounds can be obtained from the type N Kundt solutions

$$\mathrm{d}s^2 = \frac{2}{P^2}\mathrm{d}\zeta\mathrm{d}\bar{\zeta} - 2\frac{Q^2}{P^2}\mathrm{d}u\mathrm{d}v + \left[2k\frac{Q^2}{P^2}v^2 - \frac{(Q^2)_{,u}}{P^2}v + \frac{Q}{P}H(\zeta,\bar{\zeta})\delta(u))\right]\mathrm{d}u^2\,, \tag{2.16}$$

where $P = 1+\frac{1}{6}\Lambda\zeta\bar{\zeta}$, $Q = (1-\frac{1}{6}\Lambda\zeta\bar{\zeta})a + \bar{b}\zeta + b\bar{\zeta}$, $k = \frac{1}{6}\Lambda a^2 + b\bar{b}$. Here, a and b are parameters specifying various distinct canonical subclasses. We can obtain (2.5) by setting $P=Q=1$ for $\Lambda=0$.

There exists another metric form representing this family of impulsive solutions. It can be obtained from (2.7) by the inverse transformation to (2.9) for all values of U (formally), including also the impulse. If we keep the terms arising from the derivatives of step Θ, it gives us

$$\mathrm{d}s^2 = \frac{2\eta\mathrm{d}\bar{\eta} - 2\mathrm{d}u\mathrm{d}v + 2H(\eta,\bar{\eta})\delta(u)\mathrm{d}u^2}{[1+\frac{1}{6}\Lambda(\eta\bar{\eta}-uv)]^2}\,, \tag{2.17}$$

which is the metric form (2.8) we have already mentioned in the context of transformation (2.9). We can see that if we identify $\eta = Z$ on the impulse $U = 0 = u$, the function $H(Z, \bar{Z})$ is equal to $H(\eta, \bar{\eta})$. The original Brinkmann form can be easily obtained by setting $\Lambda = 0$.

2.3.2 Expanding impulsive waves

The class of vacuum Robinson–Trautman type N solutions with a cosmological constant has the family of expanding spherical gravitational impulsive waves as its limit. The standard metric of the type N Robinson-Trautman spacetime is

$$\mathrm{d}s^2 = 2\frac{r^2}{P^2}\mathrm{d}\zeta\mathrm{d}\bar{\zeta} + 2\mathrm{d}\mathrm{U}\mathrm{d}r - \left[2\epsilon + 2r(\log P)_{,\mathrm{U}} - \frac{1}{3}\Lambda r^2\right]\mathrm{d}\mathrm{U}^2\,, \tag{2.18}$$

where P is a function

$$P = (1 + \epsilon F\bar{F})(F_{,\zeta}\bar{F}_{,\bar{\zeta}})^{-\frac{1}{2}}\,, \tag{2.19}$$

where $F = F(\zeta, \mathrm{U})$ is an arbitrary complex function, and $\epsilon = -1, 0, 1$ determines the Gaussian curvature of each surface spanned by $\zeta, \bar{\zeta}$.

A family of sandwich waves, whose wave surfaces form concentric spheres at any time can be introduced by taking

$$F(\zeta, \mathrm{U}) = \zeta^{g(\mathrm{U})}\,, \tag{2.20}$$

where $g(\mathrm{U})$ is a positive function of U. In general, we have Robinson–Trautman gravitational waves with a profile determined by $g(\mathrm{U})$. These solution have a non-zero component of the Weyl tensor $\Psi_4 \propto \frac{g_{,\mathrm{U}}}{g}$. Thus the solution is conformally flat, if and only if, g is a constant.

The simplest sandwich wave is obtained by taking $g(\mathrm{U})$ as

$$\begin{aligned} g(\mathrm{U}) &= 1 && \text{for} && \mathrm{U} < 0\,,\\ g(\mathrm{U}) &= 1 - a\mathrm{U} && \text{for} && \mathrm{U} \in [0, \mathrm{U}_1]\,,\\ g(\mathrm{U}) &= 1 - a\mathrm{U}_1 && \text{for} && \mathrm{U} > \mathrm{U}_1\,, \end{aligned}$$

where a, U_1 are positive constants. This gives us $g_{,\mathrm{U}} = -a$ in the middle region, and $g_{,\mathrm{U}} = 0$ outside the wave zone. However, ahead of the sandwich wave for $\mathrm{U} > \mathrm{U}_1$, there is a topological deficit at $\zeta = 0$ and $\zeta = \infty$ (since $g < 1$) representing a cosmic string with a deficit angle $2\pi a\mathrm{U}_1$. This solution has been interpreted as a breaking of cosmic string in a conformally flat background where the string tension reduces uniformly to zero.

Using this model, we can easily perform impulsive limit by taking $\mathrm{U}_1 \to 0$, and keeping $\gamma = a\mathrm{U}_1 > 0$ fixed. This gives us the function g as

$$\begin{aligned} g(\mathrm{U}) &= 1 && \text{for} && \mathrm{U} < 0\,,\\ g(\mathrm{U}) &= 1 - \gamma && \text{for} && \mathrm{U} > 0\,. \end{aligned}$$

This can be represented using the *Heaviside step* Θ as $g(\mathrm{U}) = \exp[\, c\,\Theta(\mathrm{U})\,]$ where $c = \ln(1-\gamma) < 0$. In this case, the component of Weyl tensor is proportional to *Dirac distribution*, namely there will appear

$$\frac{g_{,\mathrm{U}}}{g} = c\,\delta(\mathrm{U})\,. \tag{2.21}$$

We have thus obtained geometry interpreted as an impulsive gravitational wave located on the expanding surface $\mathrm{U} = 0$.

Alternatively, the family of Robinson–Trautman type N metrics can be expressed in terms of García–Plebański coordinates as

$$\mathrm{d}s^2 = 2\frac{r^2}{\psi^2}\left|\mathrm{d}\xi - f\mathrm{d}\mathrm{U}\right|^2 + 2\mathrm{d}\mathrm{U}\mathrm{d}r - \left(2\epsilon - rQ - \frac{1}{3}\Lambda r^2\right)\mathrm{d}\mathrm{U}^2\,, \tag{2.22}$$

where $\psi = 1 + \epsilon\xi\bar{\xi}$, $f(\xi, \mathrm{U})$ is an arbitrary complex function, and $Q = (f_{,\xi} + \bar{f}_{,\bar{\xi}}) - 2\frac{\epsilon}{\psi}(\bar{\xi}f + \xi\bar{f})$. The transformation relating this to (2.18) is $\xi = F(\zeta, \mathrm{U})$ with $F_{,\mathrm{U}} = f(F(\zeta, \mathrm{U}), \mathrm{U})$. Making again the specific choice of F and g analogously as above, we can introduce the impulsive limit, i.e,

$$f = c\,\xi\ln\xi\,\delta(\mathrm{U})\,, \qquad Q = 2c\left(1 + \frac{1 - \epsilon\,\xi\bar{\xi}}{1 + \epsilon\,\xi\bar{\xi}}\ln|\xi|\right)\delta(\mathrm{U})\,. \tag{2.23}$$

Here, we encounter a crucial problem, the function f is quadratic in the metric (2.22), which results in the square of the Dirac δ. Formally, we can now write

$$\mathrm{d}s^2 = 2\frac{r^2}{\psi^2}\left|\mathrm{d}\xi - f(\xi)\delta(\mathrm{U})\mathrm{d}\mathrm{U}\right|^2 + 2\mathrm{d}\mathrm{U}\mathrm{d}r - \left(2\epsilon - rQ(\xi)\delta(\mathrm{U}) - \frac{1}{3}\Lambda r^2\right)\mathrm{d}\mathrm{U}^2\,. \tag{2.24}$$

This reduces for the simplest case $\Lambda = \epsilon = 0$ to

$$\mathrm{d}s^2 = 2\frac{r^2}{\psi^2}\left|\mathrm{d}\xi - f(\xi)\delta(\mathrm{U})\mathrm{d}\mathrm{U}\right|^2 + 2\mathrm{d}\mathrm{U}\mathrm{d}r + r(f_{,\xi} + \bar{f}_{,\bar{\xi}})\delta(\mathrm{U})\mathrm{d}\mathrm{U}^2\,. \tag{2.25}$$

A rigorously derived transformation relating this metric to the continuous one (2.14) as in the nonexpanding case is unknown, the formal transformation was derived in [5]. It should be our ultimate goal to solve this open problem. However, it seems more useful to assume the Robinson–Trautman metric (2.18) to bypass the δ-square problem.

2.4 Boosts and limits of infinite acceleration

There exists yet another method for the construction of particular spacetimes. It is based on boosting static sources to the speed of light for nonexpanding waves, and limits of infinite acceleration of specific static solutions, which yields special expanding impulsive solutions.

2.4.1 Nonexpanding impulsive waves

It was demonstrated in 1971 by Aichelburg and Sexl [13] that a specific impulsive gravitational *pp*-wave can be obtained by boosting the Schwarzschild black hole to the speed of light while limiting its mass to zero. Let us start with a linearised Schwarzschild metric for small values of M,

$$\mathrm{d}s^2 = -\mathrm{d}t^2 + \mathrm{d}r^2 + r^2(\mathrm{d}\theta^2 + \sin\theta^2\mathrm{d}\phi^2) + \Psi(\mathrm{d}t^2 + \mathrm{d}r^2)\,, \tag{2.26}$$

where $\Psi = \frac{2M}{r}$. We will perform the boost in Cartesian coordinates in the x direction, namely

$$t = \frac{\tilde{t} + v\tilde{x}}{\sqrt{1 - v^2}}\,, \qquad x = \frac{\tilde{x} + v\tilde{t}}{\sqrt{1 - v^2}}\,.$$

In the limit $v \to 1$, the metric takes the form

$$\mathrm{d}s^2 = -\mathrm{d}\tilde{t}^2 + \mathrm{d}\tilde{x}^2 + \mathrm{d}y^2 + \mathrm{d}z^2 + 2\lim_{v\to 1}\frac{\Psi}{1-v^2}\left(\mathrm{d}\tilde{t} + \mathrm{d}\tilde{x}\right)^2 . \tag{2.27}$$

To evaluate the limit, we use the identity

$$\lim_{v\to 1}\frac{\Psi}{1-v^2} = \delta(\tilde{t}+\tilde{x})\int_{-\infty}^{+\infty}\Psi(x)\mathrm{d}x\,,$$

which is valid in the distributional sense. As was hinted, it is necessary to scale the mass M to zero such that $8M = b_0\sqrt{1-v^2}$ where b_0 is a new constant. We obtain an impulsive *pp*-metric

$$\mathrm{d}s^2 = -\mathrm{d}\tilde{t}^2 + \mathrm{d}\tilde{x}^2 + \mathrm{d}y^2 + \mathrm{d}z^2 + H\delta(\tilde{t}+\tilde{x})\left(\mathrm{d}\tilde{t} + \mathrm{d}\tilde{x}\right)^2 , \tag{2.28}$$

where

$$H = \frac{1}{2}b_0\int_{-\infty}^{+\infty}\left(x^2+y^2+z^2\right)^{-\frac{1}{2}}\mathrm{d}x\,.$$

This is the famous Aichelburg–Sexl solution which represents an axially symmetric impulsive gravitational wave in Minkowski space generated by a single null monopole located on the axis $y^2 + z^2 = 0$.

2.4.2 Expanding impulsive waves

Now, we turn our attention to infinitely accelerating static sources to generate expanding impulsive waves. We shall present the solution described by Bičák, Hoenselaers, and Schmidt [22].

In general, the boost-rotation symmetric spacetimes can be described by the line element

$$\mathrm{d}s^2 = e^{\lambda}\mathrm{d}\rho^2 + \rho^2 e^{-\mu}\mathrm{d}\phi^2 + (\zeta^2-\tau^2)^{-1}\left[e^{\lambda}(\zeta\mathrm{d}\zeta - \tau\mathrm{d}\tau)^2 - e^{\mu}(\zeta\mathrm{d}\tau - \tau\mathrm{d}\zeta)^2\right] , \tag{2.29}$$

where function μ and λ depend only on $\zeta^2 - \tau^2$ and ρ^2. In our case, we start with the Bonnor–Swaminarayan solutions which generally contain five arbitrary constants m_1, m_2, A_1, A_2 and B. They determine masses and uniform accelerations of two pairs of particles, and B the singularity structure on the axis of symmetry $\rho = 0$. Of particular interest are special cases described by Bičák, Hoenselaers and Schmidt, which represent only one pair of particles of the Curzon-Chazy type accelerating in opposite directions. For such solutions, the metric functions can be written as

$$\begin{aligned}\mu &= -\frac{2m}{AR} + 4mA + B\,,\\ \lambda &= -\frac{m^2}{A^2R^4}\rho^2(\zeta^2-\tau^2) + \frac{2mA}{R}(\rho^2+\zeta^2-\tau^2) + B\,,\end{aligned}$$

where $R = \frac{1}{2}\sqrt{(\rho^2+\zeta^2-\tau^2-A^{-2})^2 + 4A^{-2}\rho^2}$. For $B = 0$, the axis $\rho = 0$ is regular between the pair of the particles; however, these are connected to infinity by two semi-infinite strings which cause their acceleration. On the other hand, taking $B = -4mA$, there is a finite expanding strut between the particles.

These solutions were investigated in the limit of infinite acceleration $A \to \infty$. It is necessary to scale the mass parameter m to zero such that the "monopole moment" $M_0 = -4mA$ remains constant. We get

$$\mu = B - M_0\,,$$
$$\lambda = B\,\mathrm{sign}\left(\rho^2 + \zeta^2 - \tau^2\right) M_0\,.$$

The resulting spacetime is locally flat everywhere except on the sphere $\rho^2 + \zeta^2 = \tau^2$. Therefore, it describes an expanding spherical impulsive gravitational wave generated by two particles that move apart at the speed of light in the Minkowski background, and which are either connected by two semi-infinite strings ($B = 0$), or to each other by expanding strut ($B = M_0$). Performing the transformation

$$\rho = \frac{1}{2}(v-u)\,, \qquad \tau = \pm\frac{1}{2}(v+u)\,, \qquad \zeta = \frac{1}{2}(v+u)\sinh\chi\,,$$

we get

$$\mathrm{d}s^2 = \frac{1}{4}(v-u)^2 e^{-\mu}\mathrm{d}\phi^2 + \frac{1}{4}(v+u)^2 e^{\mu}\mathrm{d}\chi^2 - e^{\lambda}\mathrm{d}v\mathrm{d}u\,, \tag{2.30}$$

where

$$\mu = -M_0\,, \qquad \lambda = [\Theta(vu) - \Theta(-vu)]M_0$$

for two receding strings, or

$$\mu = 0\,, \qquad \lambda = 2\Theta(vu)M_0$$

for the expanding strut. In both cases, μ is a constant, but λ has a step of $2M_0$ on the null cone $uv = 0$.

Interestingly, a particular transformation relates this metric with (2.13). In the region where μ, λ are constant. The transformation

$$\mathrm{U} = -ue^{\lambda+\mu/2}\,, \qquad \mathrm{V} = \frac{1}{2}ve^{-\mu/2}\,, \qquad \psi = \chi e^{\mu}$$

brings the metric (2.30) into the form

$$\mathrm{d}s^2 = \left(\mathrm{V} + \frac{1}{2}P\mathrm{U}\right)^2 \mathrm{d}\phi^2 + \left(\mathrm{V} - \frac{1}{2}P\mathrm{U}\right)^2 \mathrm{d}\psi^2 + 2\mathrm{d}\mathrm{U}\mathrm{d}\mathrm{V}\,, \tag{2.31}$$

where $P = e^{-\lambda-\mu}$. The solution for two receding strings can be written in the form

$$P = \Theta(-\mathrm{U}) + e^{2M_0}\Theta(\mathrm{U})\,.$$

The metric obtained represents an impulsive spherical gravitational wave propagating in Minkowski space. Outside the impulse ($\mathrm{U} > 0$), there are two receding strings characterized by a deficit angle $(1-\beta)2\pi$ (where $\beta = e^{2M_0}$). The complementary solution for an expanding strut can be written as

$$P = e^{-2M_0}\Theta(-\mathrm{U}) + \Theta(\mathrm{U})\,.$$

In this case, there is a string with the deficit angle $(1-\beta^{-1})2\pi$ inside the impulse ($\mathrm{U} < 0$). By further transforming

$$Z = \frac{1}{\sqrt{2}}\left(\psi + i\phi\right)\,,$$

we get the metric (2.14) for $\Lambda = 0$ and $\epsilon = 0$, namely

$$\mathrm{d}s^2 = 2\left|\mathrm{V}\mathrm{d}Z + \mathrm{U}H\mathrm{d}\bar{Z}\right|^2 + 2\mathrm{d}\mathrm{U}\mathrm{d}\mathrm{V}\,, \qquad \text{where} \qquad H = -\frac{1}{2}\beta^2\,.$$

Finally, performing a different transformation of the metric (2.30) in the region with $u > 0,\ v > 0$, namely

$$\begin{aligned}
\mathrm{U} &= -\frac{uv}{u+v}\exp\left[\frac{\lambda}{2} - \chi e^{(\mu-\lambda)/2}\right]\,,\\
\mathrm{V} &= \frac{1}{2}(u+v)\exp\left[\frac{\lambda}{2} + \chi e^{(\mu-\lambda)/2}\right]\,,\\
Z &= \frac{1}{\sqrt{2}}\frac{v-u}{v+u}\exp\left[-\chi^{(\mu-\lambda)/2} + i\phi^{-(\mu+\lambda)/2}\right]\,,
\end{aligned}$$

we obtain the metric (2.4) for $\Lambda = 0$, $\epsilon = 0$, i.e.,

$$\mathrm{d}s^2 = 2\mathrm{V}^2\mathrm{d}Z\mathrm{d}\bar{Z} + 2\mathrm{d}\mathrm{U}\mathrm{d}\mathrm{V}\,.$$

The above metrics can be matched continuously across the null cone $\mathrm{U} = 0$, and we obtain a particular case of (2.14) for $\Lambda = 0$, $\epsilon = 0$, and $H = -\frac{1}{2}\beta^2$, see [11].

3. Geodesics in impulsive gravitational waves

In this chapter, we would like to describe the behavior of geodesics in impulsive gravitational waves, and how it can be used to analyze spacetime geometry. Moreover, the geodesics and their properties are crucial tools for rigorously constructing the continuous line elements of the impulsive spacetimes. It is well established in the nonexpanding case; however, the expanding case is still not completely understood. The thesis should be our first step in this direction.

3.1 Nonexpanding impulsive waves

In this section, we are going to focus on nonexpanding impulsive waves. For more clarity and further usefulness, we will work with Λ set to zero, i.e., with impulses propagating on a flat Minkowski background.

Geodesics in Minkowski space with impulsive *pp*-waves can be approached as refracted straight lines with a jump in the v-direction. However, as we will see, the geodesic equation in the standard coordinates (distributional limit) introduces specific problems since it contains nonlinear distributional terms. These are not well defined in the classical theory of distributions, and were typically solved using methods of Colombeau's algebras [23, 24, 25].

We can employ the existence of C^1 global geodesics as an alternative approach to studying the geodesic equations and their implications. This assumption was justified and proven to be rigorous via Fillipov's solution concept [26] in [18].

3.1.1 Deriving the continuous coordinates

Firstly, we will follow the approach of Kunzinger and Steinbauer [20, 27], and use the *real* distributional form of the metric (2.17) to solve the equations of geodesics. The metric explicitly reads

$$\mathrm{d}s^2 = \delta(u)H(x^i)\mathrm{d}u^2 - \mathrm{d}u\mathrm{d}v + (\mathrm{d}x^i)^2\,, \tag{3.1}$$

where $i = 1, 2$ denotes the transverse coordinates. We find the geodesic equations in the form

$$\begin{aligned} \ddot{u}(\alpha) &= 0\,, \\ \ddot{v}(\alpha) &= H(x^i(\alpha))\dot{\delta}(\alpha) + 2\partial_j H(x^i(\alpha))\dot{x}^j(\alpha)\delta(\alpha)\,, \\ \ddot{x}^i(\alpha) &= \frac{1}{2}\partial_i H(x^j(\alpha))\delta(\alpha)\,, \end{aligned} \tag{3.2}$$

where the *dot* denotes derivative with respect to the parameter α. From the first equation, we see that u is a linear function of α, so we can use this coordinate as an affine parameter, rewriting the latter equations by substituting u for α. We can see that the equation for v involves a derivative of the Dirac δ distribution, thus we cannot expect it to be continuous. We now transfer to the Colombeau framework, and invoke the regularisation method. Knowledge of geodesics allows

us to extract the continuous coordinate system. In particular, we have to choose a specific class of geodesics such that their initial speed, i.e., in front of the impulse, is non-vanishing only in the u-direction. The set of initial data in the case of the regularised equation, see [20] for more details, is thus $x^i_\epsilon = x^i_0$, $v_\epsilon = v_0$, and $\dot{x}^i_\epsilon = 0 = \dot{v}_\epsilon$. The solution acquired by integrating the regularised equation has a distributional limit

$$\begin{aligned} x^i_\epsilon(x^j_0, u) &\to x^i_0 + \frac{1}{2}\partial_i H(x^j_0)u_+ \,, \\ v_\epsilon(v_0, x^j_0, u) &\to v_0 + H(x^j_0)\theta(u) + \frac{1}{4}\partial_i H(x^j_0)\partial^i H(x^j_0)u_+ \,. \end{aligned} \tag{3.3}$$

Now, we can use these geodesics as new coordinate lines. Obviously, these lines are uniquely determined by the *initial data*, which then naturally play the role of new coordinates continuous across the impulse. If we compare the resulting limit with the transformation (2.9), we see they are the same apart from having real instead of complex transverse coordinates.

In the case of expanding impulsive gravitational waves, an analogous transformation to (2.9) between the distributional form – probably the most convenient expressions are (2.18) or (2.24) – and continuous form of the metric (2.14) has not yet been explicitly found in a rigorous way. However, it is of extreme importance to understand geodesic behavior.

3.1.2 Refraction of geodesics

Our next step is to look at geodesics crossing the impulse. As was mentioned before, it has been shown that the geodesic equation has a unique C^1 solution if the initial data are not set on the impulse $u = 0$. To carry out this C^1-matching procedure, we start with the unique globally defined C^1-geodesics in the continuous metric [18]. By converting these geodesics into null conformally flat coordinates, which are well-suited to the background spacetime, and doing so separately on both sides of the wave surface, we derive the matching conditions for their positions. Performing the same procedure for their derivatives we obtain refraction formulae for velocities across the impulse. In particular, we consider geodesics

$$U = U(\tau)\,, \qquad V = V(\tau)\,, \qquad Z = Z(\tau)$$

in the continuous coordinates. As they are globally defined C^1-curves, positions and velocities at the instant of the interaction with the impulse must be equal on both sides. Thus, by employing the transformation (2.9) and its derivative separately in front of and behind the impulse, we can express the *refraction formulae* for the geodesics crossing the impulse at $U = 0$ as

$$\begin{aligned} &u_i^- = 0 = u_i^+\,, && \dot{u}_i^- = \dot{u}_i^+\,, \\ &v_i^- = v_i^+ - H_i\,, && \dot{v}_i^- = \dot{v}_i^+ - H_{i,Z}\dot{\eta}_i^+ - H_{i,\bar{Z}}\dot{\bar{\eta}}_i^+ - H_i + \dot{u}_i^+ H_{i,Z}H_{i,\bar{Z}}\,, \\ &\eta_i^- = \eta_i^+\,, && \dot{\eta}_i^- = \dot{\eta}_i^+ - \dot{u}_i^+ H_{i,Z}\,. \end{aligned} \tag{3.4}$$

We observe that they suffer a jump in the v-direction, and are refracted both in the v-direction and perpendicular spatial directions.

Writing the refraction formulae using the real spatial coordinates as in [28], we observe that they match the solution we got for geodesics (3.3) derived in the distributional form. This fully corresponds to the rigorous procedure used for the continuous coordinate construction.

3.2 Expanding impulsive waves

Here, we are going to summarize what is known about the description of geodesics in expanding impulsive waves. The first thing to point out is that the possible distributional form of the metric contains a square of the δ distribution. Therefore, rigorous formulation of its regularised version seems to be very difficult or even impossible. The distributional form with vanishing Λ reads

$$\begin{aligned} \mathrm{d}s^2 = 2\mathrm{d}u\mathrm{d}v + 2\frac{v^2}{\psi^2}\left|\mathrm{d}\eta - F\delta(u)\mathrm{d}u\right|^2 - 2\epsilon\mathrm{d}u^2 \\ + v\left[(F_{,\eta} + \bar{F}_{,\bar{\eta}}) - \frac{2\epsilon}{\psi}(F\bar{\eta} + \bar{F}\eta)\right]\delta(u)\mathrm{d}u^2\,, \end{aligned} \tag{3.5}$$

where $\psi = 1 + \epsilon\eta\bar{\eta}$, and $F(\eta)$ is an arbitrary function that is related to the warp function $h(Z)$ as $F = Z_{inv} - Z$, where Z_{inv} is inverse to (2.10). This is given in the original null background coordinates. It could be useful to find such an expression in the more adapted null cone coordinates, which should be closer to the continuous coordinate form of the metric (2.14).

As an alternative attempt to describe geodesics interacting with expanding impulses, we explicitly derive the geodesic equations using the continuous form of the metric (2.14). This will allow us to show that they admit a special family of solutions. For simplicity, we assume $\Lambda = 0$. Then the components of the metric are

$$\begin{aligned} g_{\mathrm{UU}} &= -2\epsilon\,, \\ g_{\mathrm{UV}} &= 1\,, \\ g_{ZZ} &= 2\mathrm{V}\mathrm{U}_+H\,, \\ g_{Z\bar{Z}} &= \frac{\mathrm{V}^2}{p^2} + \mathrm{U}_+^2\,p^2|H|^2\,. \end{aligned} \tag{3.6}$$

It is useful to express their derivatives

$$\begin{aligned} g_{ZZ\,,\mathrm{U}} &= 2\mathrm{V}H\mathrm{U}_{+,\mathrm{U}}\,, \\ g_{ZZ\,,\mathrm{V}} &= 2H\mathrm{U}_+\,, \\ g_{ZZ\,,Z} &= 2V\mathrm{U}_+H_{,Z}\,, \\ g_{Z\bar{Z}\,,\mathrm{U}} &= p^2H\bar{H}\,\mathrm{U}_{+,\mathrm{U}}^2\,, \\ g_{Z\bar{Z}\,,\mathrm{V}} &= \frac{2V}{p^2}\,, \\ g_{Z\bar{Z}\,,Z} &= -\frac{2\epsilon\bar{Z}V^2}{p^3} + \mathrm{U}_+^2\left(2p\epsilon\bar{Z}H\bar{H} + p^2H_{,Z}\bar{H} + p^2H\bar{H}_{,Z}\right). \end{aligned}$$

Now, based on the non-zero components of the Christoffel symbols [19], we

can write down the symbolic form of geodesic equations,

$$\begin{aligned}
0 &= \ddot{\mathrm{U}} + \Gamma^{\mathrm{U}}{}_{ZZ}\,\dot{Z}\dot{Z} + \Gamma^{\mathrm{U}}{}_{\bar{Z}\bar{Z}}\,\dot{\bar{Z}}\dot{\bar{Z}} + 2\Gamma^{\mathrm{U}}{}_{\bar{Z}Z}\,\dot{\bar{Z}}\dot{Z}\,,\\
0 &= \ddot{\mathrm{V}} + \Gamma^{\mathrm{V}}{}_{ZZ}\,\dot{Z}\dot{Z} + \Gamma^{\mathrm{V}}{}_{\bar{Z}\bar{Z}}\,\dot{\bar{Z}}\dot{\bar{Z}} + 2\Gamma^{\mathrm{V}}{}_{\bar{Z}Z}\,\dot{\bar{Z}}\dot{Z}\,,\\
0 &= \ddot{Z} + 2\Gamma^{Z}{}_{Z\mathrm{U}}\,\dot{Z}\dot{U} + 2\Gamma^{Z}{}_{Z\mathrm{V}}\,\dot{Z}\dot{V} + \Gamma^{Z}{}_{ZZ}\,\dot{Z}\dot{Z}\\
&\qquad + 2\Gamma^{Z}{}_{\bar{Z}Z}\,\dot{\bar{Z}}\dot{Z} + 2\Gamma^{Z}{}_{\bar{Z}\mathrm{U}}\,\dot{\bar{Z}}\dot{U} + 2\Gamma^{Z}{}_{\bar{Z}\mathrm{V}}\,\dot{\bar{Z}}\dot{V}\,,
\end{aligned} \tag{3.7}$$

where *dot* denotes the derivative by parameter τ. The geodesic equations are now fully coupled, so sadly we can not take U as an affine parameter. The full geodesic equation for arbitrary Λ can be found in [19] where Podolský, Sämann, Steinbauer, and Švarc investigated the uniqueness and continuity of the geodesics using Filippov's concept of solution [26]. Their result justified the C^1-matching procedure, which we will discuss in the next section.

With a quick look at the equations, we see that it admits a globally privileged family of geodesics of the form

$$\begin{aligned}
Z &= Z_i = \text{const}\,,\\
\mathrm{U} &= \dot{\mathrm{U}}_i(\tau - \tau_i)\,,\\
\mathrm{V} &= \dot{\mathrm{V}}_i(\tau - \tau_i) + \mathrm{V}_i\,,
\end{aligned} \tag{3.8}$$

where τ_i corresponds to the instant of interaction with the impulse.

In the conformally flat coordinates, the general form of the geodesics is

$$\begin{aligned}
v^{\pm} &= \dot{v}_i^{\pm}(\tau - \tau_i) + v_i^{\pm}\,,\\
u^{\pm} &= \dot{u}_i^{\pm}(\tau - \tau_i) + u_i^{\pm}\,,\\
\eta^{\pm} &= \dot{\eta}_i^{\pm}(\tau - \tau_i) + \eta_i^{\pm}\,,
\end{aligned} \tag{3.9}$$

where analogously τ_i is the value of the affine parameter when the impulse hits the test particle. Here, the space outside the null cone is denoted by the superscript $^+$, and the subspace inside by the superscript $^-$. Trivially, we can also express the geodesics in natural Minkowski coordinates, namely

$$\begin{aligned}
t^{+} &= \gamma\tau\,,\\
x^{+} &= \dot{x}_i(\tau - \tau_i) + x_i\,,\\
y^{+} &= \dot{y}_i(\tau - \tau_i) + y_i\,,\\
z^{+} &= \dot{z}_i(\tau - \tau_i) + z_i\,.
\end{aligned} \tag{3.10}$$

with normalisation $\gamma = \sqrt{\dot{x}_i^2 + \dot{y}_i^2 + \dot{z}_i^2 - e}$ where $e = -1$ for timelike, $e = 1$ for spacelike, and $e = 0$ for null geodesics, respectively. The interaction is given by $\tau_i = \sqrt{x_i^2 + y_i^2 + z_i^2}/\gamma$, more details can be found in [29, 16]. Now, we will focus on the refraction formulae.

3.2.1 Refraction formulae

We will derive them in the same manner as for the nonexpanding case. Following [30], we use the parameterization (1.6) inside the null cone, and (2.10) outside the null cone. We proceed by noting that the geodesics are C1 curves. It means

that the corresponding functions $Z(\tau), \mathrm{V}(\tau), \mathrm{U}(\tau)$ and their first derivatives with respect to the affine parameter τ, evaluated at the interaction time $\tau = \tau_i$, are continuous across the impulse. Assuming this, the constants

$$\begin{aligned} Z_i &= Z(\tau_i)\,, \quad & \mathrm{V}_i &= \mathrm{V}(\tau_i)\,, \quad & \mathrm{U}_i &= \mathrm{U}(\tau_i) = 0\,, \\ \dot{Z}_i &= \dot{Z}(\tau_i)\,, \quad & \dot{\mathrm{V}}_i &= \dot{\mathrm{V}}(\tau_i)\,, \quad & \dot{\mathrm{U}}_i &= \dot{\mathrm{U}}(\tau_i)\,, \end{aligned}$$

describing positions and velocities at τ_i have the same value at both sides of the impulse. Taking the limits, we get

$$\begin{aligned} v_i^+ &= A\mathrm{V}_i\,, & \dot{v}_i^+ &= A\dot{\mathrm{V}}_i - D\dot{\mathrm{U}}_i + (A_{,Z}\dot{Z}_i + A_{,\bar{Z}}\dot{\bar{Z}}_i)\mathrm{V}_i\,, \\ u_i^+ &= B\mathrm{V}_i\,, & \dot{u}_i^+ &= B\dot{\mathrm{V}}_i - E\dot{\mathrm{U}}_i + (B_{,Z}\dot{Z}_i + B_{,\bar{Z}}\dot{\bar{Z}}_i)\mathrm{V}_i\,, \\ \eta_i^+ &= C\mathrm{V}_i\,, & \dot{\eta}_i^+ &= C\dot{\mathrm{V}}_i - F\dot{\mathrm{U}}_i + (C_{,Z}\dot{Z}_i + C_{,\bar{Z}}\dot{\bar{Z}}_i)\mathrm{V}_i\,, \end{aligned} \tag{3.11}$$

and inside the impulse

$$\begin{aligned} v_i^- &= \frac{\mathrm{V}_i}{p}\,, & \dot{v}_i^- &= -\frac{\epsilon \mathrm{V}_i}{p^2}(Z_i\dot{\bar{Z}}_i + \bar{Z}_i\dot{Z}_i) + \frac{\dot{\mathrm{V}}_i}{p} - \epsilon\dot{\mathrm{U}}_i\,, \\ u_i^- &= \frac{Z_i\bar{Z}_i}{p}\mathrm{V}_i\,, & \dot{u}_i^- &= \frac{\mathrm{V}_i}{p^2}(Z_i\dot{\bar{Z}}_i + \bar{Z}_i\dot{Z}_i) + \frac{Z_i\bar{Z}_i}{p}\dot{\mathrm{V}}_i - \dot{\mathrm{U}}_i\,, \\ \eta_i^- &= \frac{Z_i}{p}\mathrm{V}_i\,, & \dot{\eta}_i^- &= \frac{\mathrm{V}_i}{p^2}(\dot{Z}_i - \epsilon Z_i Z_i\dot{\bar{Z}}_i) + \frac{Z_i}{p}\dot{\mathrm{V}}_i\,. \end{aligned} \tag{3.12}$$

To express the $^-$ parameters in terms of the $^+$ parameters, we have to invert (3.11), and invoke the transformation identities (2.12) and their derivatives. That yields

$$\begin{aligned} h(Z_i) &= \frac{\eta_i^+}{v_i^+}\,, \\ \mathrm{V}_i &= \frac{v_i^+}{A} = \frac{u_i^+}{B} = \frac{\eta_i^+}{C}\,, \\ \dot{Z}_i &= \frac{p^2}{\mathrm{V}_i}\left(\bar{C}_{,\bar{Z}}\dot{\eta}_i^+ + C_{,\bar{Z}}\dot{\bar{\eta}}_i^+ - A_{,\bar{Z}}\dot{u}_i^+ - B_{,\bar{Z}}\dot{v}_i^+\right)\,, \\ \dot{\mathrm{V}}_i &= D\dot{u}_i^+ + E\dot{v}_i^+ - \bar{F}\dot{\eta}_i^+ - F\dot{\bar{\eta}}_i^+ + 2\epsilon\dot{\mathrm{U}}_i\,, \\ \dot{\mathrm{U}}_i &= \frac{1}{\mathrm{V}_i}\left(\bar{\eta}_i^+\dot{\eta}_i^+ + \eta_i^+\dot{\bar{\eta}}_i^+ - v_i^+\dot{u}_i^+ - u_i^+\dot{v}_i^+\right)\,. \end{aligned} \tag{3.13}$$

Now we only input these into (3.12). For the positions we get

$$\begin{aligned} v_i^- &= |h'|v_i^+\,, \\ u_i^- &= |h'|\frac{|Z_i|^2}{|h|^2}\,u_i^+\,, \\ \eta_i^- &= |h'|\frac{Z_i}{h}\,\eta_i^+\,, \end{aligned} \tag{3.14}$$

and for velocities

$$\begin{aligned} \dot{v}_i^- &= b_v\dot{v}_i^+ + a_v\dot{u}_i^+ + \bar{c}_v\dot{\eta}_i^+ + c_v\dot{\bar{\eta}}_i^+\,, \\ \dot{u}_i^- &= b_u\dot{v}_i^+ + a_u\dot{u}_i^+ + \bar{c}_u\dot{\eta}_i^+ + c_u\dot{\bar{\eta}}_i^+\,, \\ \dot{\eta}_i^- &= b_\eta\dot{v}_i^+ + a_\eta\,\dot{u}_i^+ + \bar{c}_\eta\,\dot{\eta}_i^+ + c_\eta\,\dot{\bar{\eta}}_i^+\,, \end{aligned} \tag{3.15}$$

where

$$
\begin{aligned}
b_{_v} &= \frac{|h|^2}{4|h'|}\left|\frac{h''}{h'} - 2\frac{h'}{h}\right|^2, \\
a_{_v} &= \frac{1}{4|h'|}\left|\frac{h''}{h'}\right|^2, \\
c_{_v} &= -\frac{h}{4|h'|}\left(\frac{h''}{h'} - 2\frac{h'}{h}\right)\frac{\bar{h}''}{\bar{h}'},
\end{aligned}
\tag{3.16}
$$

$$
\begin{aligned}
b_{_u} &= \frac{|h|^2}{|h'|}\left|1 + \frac{Z_i}{2}\left(\frac{h''}{h'} - 2\frac{h'}{h}\right)\right|^2, \\
a_{_u} &= \frac{1}{|h'|}\left|1 + \frac{Z_i}{2}\frac{h''}{h'}\right|^2, \\
c_{_u} &= -\frac{h}{|h'|}\left[1 + \frac{Z_i}{2}\left(\frac{h''}{h'} - 2\frac{h'}{h}\right)\right]\left[1 + \frac{\bar{Z}_i}{2}\frac{\bar{h}''}{\bar{h}'}\right].
\end{aligned}
\tag{3.17}
$$

$$
\begin{aligned}
b_{\eta} &= \frac{|h|^2}{2|h'|}\left[1 + \frac{Z_i}{2}\left(\frac{h''}{h'} - 2\frac{h'}{h}\right)\right]\left(\frac{\bar{h}''}{\bar{h}'} - 2\frac{\bar{h}'}{\bar{h}}\right), \\
a_{\eta} &= \frac{1}{2|h'|}\left(1 + \frac{Z_i}{2}\frac{h''}{h'}\right)\frac{\bar{h}''}{\bar{h}'}, \\
\bar{c}_{\eta} &= -\frac{\bar{h}}{2|h'|}\left(1 + \frac{Z_i}{2}\frac{h''}{h'}\right)\left(\frac{\bar{h}''}{\bar{h}'} - 2\frac{\bar{h}'}{\bar{h}}\right), \\
c_{\eta} &= -\frac{h}{2|h'|}\left[1 + \frac{Z_i}{2}\left(\frac{h''}{h'} - 2\frac{h'}{h}\right)\right]\frac{\bar{h}''}{\bar{h}'}.
\end{aligned}
\tag{3.18}
$$

All of these coefficients are constants acquired by evaluating the function h and its derivatives at the instant of the interaction, i.e., at $Z = Z_i$. In the simplest trivial case with $h(Z) = Z$, we get an identity, which corresponds to the fact that the H function in the continuous coordinates vanishes and there is no impulse in the spacetime [30].

Finally, using the transformation between natural coordinates and null coordinates, we can rewrite the expressions (3.14) and (3.15) using the natural Minkowski coordinates, giving us

$$
\begin{aligned}
x_i^- &= |h'|\frac{Z_i + \bar{Z}_i}{h + \bar{h}}x_i^+, \\
y_i^- &= |h'|\frac{Z_i - \bar{Z}_i}{h - \bar{h}}y_i^+, \\
z_i^- &= |h'|\frac{|Z_i|^2 - 1}{|h|^2 - 1}z_i^+, \\
t_i^- &= |h'|\frac{|Z_i|^2 + 1}{|h|^2 + 1}t_i^+,
\end{aligned}
\tag{3.19}
$$

for positions and

$$\begin{aligned}
\dot{x}_i^- &= a_x \dot{x}_i^+ + b_x \dot{y}_i^+ + c_x \dot{z}_i^+ + d_x \dot{t}_i^+ \,, \\
\dot{y}_i^- &= a_y \dot{x}_i^+ + b_y \dot{y}_i^+ + c_y \dot{z}_i^+ + d_y \dot{t}_i^+ \,, \\
\dot{z}_i^- &= a_z \dot{x}_i^+ + b_z \dot{y}_i^+ + c_z \dot{z}_i^+ + d_z \dot{t}_i^+ \,, \\
\dot{t}_i^- &= a_t \dot{x}_i^+ + b_t \dot{y}_i^+ + c_t \dot{z}_i^+ + d_t \dot{t}_i^+ \,,
\end{aligned} \tag{3.20}$$

for velocities. The coefficients in (3.20) are combinations of coefficients in (3.15),

$$\begin{aligned}
a_x &= \frac{1}{2}\left(c_\eta + c_{\bar{\eta}} + \bar{c}_\eta + \bar{c}_{\bar{\eta}}\right), \\
b_x &= \frac{i}{2}\left(-c_\eta - c_{\bar{\eta}} + \bar{c}_\eta + \bar{c}_{\bar{\eta}}\right), \\
c_x &= \frac{1}{2}\left(-a_\eta - a_{\bar{\eta}} + b_\eta + b_{\bar{\eta}}\right), \\
d_x &= \frac{1}{2}\left(a_\eta + a_{\bar{\eta}} + b_\eta + b_{\bar{\eta}}\right),
\end{aligned}$$

$$\begin{aligned}
a_y &= \frac{1}{2\,i}\left(c_\eta - c_{\bar{\eta}} + \bar{c}_\eta - \bar{c}_{\bar{\eta}}\right), \\
b_y &= \frac{1}{2}\left(-c_\eta + c_{\bar{\eta}} + \bar{c}_\eta - \bar{c}_{\bar{\eta}}\right), \\
c_y &= \frac{1}{2\,i}\left(-a_\eta + a_{\bar{\eta}} + b_\eta - b_{\bar{\eta}}\right), \\
d_y &= \frac{1}{2\,i}\left(a_\eta - a_{\bar{\eta}} + b_\eta - b_{\bar{\eta}}\right),
\end{aligned} \tag{3.21}$$

$$\begin{aligned}
a_z &= \frac{1}{2}\left(-c_u - \bar{c}_u + c_v + \bar{c}_v\right), \\
b_z &= \frac{i}{2}\left(c_u - \bar{c}_u - c_v + \bar{c}_v\right), \\
c_z &= \frac{1}{2}\left(a_u - a_v - b_u + b_v\right), \\
d_z &= \frac{1}{2}\left(-a_u + a_v - b_u + b_v\right),
\end{aligned}$$

$$\begin{aligned}
a_t &= \frac{1}{2}\left(c_u + \bar{c}_u + c_v + \bar{c}_v\right), \\
b_t &= \frac{i}{2}\left(-c_u + \bar{c}_u - c_v + \bar{c}_v\right), \\
c_t &= \frac{1}{2}\left(-a_u - a_v + b_u + b_v\right), \\
d_t &= \frac{1}{2}\left(a_u + a_v + b_u + b_v\right).
\end{aligned}$$

In practice, we have to choose our warp function $h(Z)$. In the next chapter, we will work with these relations and visualize the resulting behavior of geodesics when crossing the impulse for a spacetime with one cosmic string, i.e., $h(Z) = Z^{1-\delta}$, where δ is a real positive constant, and $\delta < 1$.

3.2.2 Privileged geodesics with $Z = \text{const}$

For our privileged geodesics (3.8) the formulae get rather smooth. Again, we use the parameterization (1.6) inside the null cone and (2.10) outside the null cone. However, now $Z = Z_i = Z_0$ is constant along the geodesics, so the velocities will be different. The refraction formulae for the privileged geodesics were reduced to

$$\begin{aligned} v_i^+ &= A\mathrm{V}_i\,, & \dot{v}_i^+ &= A\dot{\mathrm{V}}_i - D\dot{\mathrm{U}}_i\,,\\ u_i^+ &= B\mathrm{V}_i\,, & \dot{u}_i^+ &= B\dot{\mathrm{V}}_i - E\dot{\mathrm{U}}_i\,,\\ \eta_i^+ &= C\mathrm{V}_i\,, & \dot{\eta}_i^+ &= C\dot{\mathrm{V}}_i - F\dot{\mathrm{U}}_i\,, \end{aligned} \tag{3.22}$$

outside the impulse. The constants A, B, C, D, E and F are evaluated at the value $Z = Z_i = Z_0$. Inside the impulse we have

$$\begin{aligned} v_i^- &= \frac{\mathrm{V}_i}{p}\,, & \dot{v}_i^- &= \frac{\dot{\mathrm{V}}_i}{p} - \epsilon\dot{\mathrm{U}}_i\,,\\ u_i^- &= \frac{Z_i\bar{Z}_i}{p}\mathrm{V}_i\,, & \dot{u}_i^- &= \frac{Z_i\bar{Z}_i}{p}\dot{\mathrm{V}}_i - \dot{\mathrm{U}}_i\,,\\ \eta_i^- &= \frac{Z_i}{p}\mathrm{V}_i\,, & \dot{\eta}_i^- &= \frac{Z_i}{p}\dot{\mathrm{V}}_i\,. \end{aligned} \tag{3.23}$$

We proceed in the same manner as for general geodesics, inverting relations (3.22) by using the identities (2.12), to express the $^-$ parameters in the terms of the $^+$ parameters. We get

$$\begin{aligned} h(Z_i) &= \frac{\eta_i^+}{v_i^+}\,, \qquad \mathrm{V}_i = \frac{v_i^+}{A} = \frac{u_i^+}{B} = \frac{\eta_i^+}{C}\,,\\ \dot{\mathrm{V}}_i &= D\dot{u}_i^+ + E\dot{v}_i^+ - \bar{F}\dot{\eta}_i^+ - F\dot{\bar{\eta}}_i^+ + 2\epsilon\dot{\mathrm{U}}_i\,,\\ \dot{\mathrm{U}}_i &= -A\dot{u}_i^+ - B\dot{v}_i^+ + \bar{C}\dot{\eta}_i^+ + C\dot{\bar{\eta}}_i^+\,. \end{aligned} \tag{3.24}$$

Now we input these into (3.23) and get

$$\begin{aligned} v_i^- &= |h'|v_i^+\,,\\ u_i^- &= |h'|\frac{|Z_i|^2}{|h|^2}\,u_i^+\,,\\ \eta_i^- &= |h'|\frac{Z_i}{h}\,\eta_i^+\,, \end{aligned} \tag{3.25}$$

and for velocities

$$\begin{aligned} \dot{v}_i^- &= b_v^0\dot{v}_i^+ + a_v^0\dot{u}_i^+ + \bar{c}_v^0\dot{\eta}_i^+ + c_v^0\dot{\bar{\eta}}_i^+\,,\\ \dot{u}_i^- &= b_u^0\dot{v}_i^+ + a_u^0\dot{u}_i^+ + \bar{c}_u^0\dot{\eta}_i^+ + c_u^0\dot{\bar{\eta}}_i^+\,,\\ \dot{\eta}_i^- &= b_\eta^0\dot{v}_i^+ + a_\eta^0\,\dot{u}_i^+ + \bar{c}_\eta^0\,\dot{\eta}_i^+ + c_\eta^0\,\dot{\bar{\eta}}_i^+\,, \end{aligned} \tag{3.26}$$

where

$$\begin{aligned} b_v^0 &= \frac{1}{p}(E - 2\epsilon B) + \epsilon B\,,\\ a_v^0 &= \frac{1}{p}(D - 2\epsilon A) + \epsilon A\,,\\ c_v^0 &= -\frac{1}{p}(F - 2\epsilon C) - \epsilon C\,, \end{aligned} \tag{3.27}$$

$$
\begin{aligned}
b_u^0 &= \frac{|Z_i|^2}{p}(E - 2\epsilon B) + B\,, \\
a_u^0 &= \frac{|Z_i|^2}{p}(D - 2\epsilon A) + A\,, \\
c_u^0 &= -\frac{|Z_i|^2}{p}(F - 2\epsilon C) - C\,,
\end{aligned}
\tag{3.28}
$$

$$
\begin{aligned}
b_\eta^0 &= \frac{Z_i}{p}(E - 2\epsilon B)\,, \\
a_\eta^0 &= \frac{Z_i}{p}(D - 2\epsilon A)\,, \\
\bar{c}_\eta^0 &= -\frac{Z_i}{p}(\bar{F} - 2\epsilon \bar{C})\,, \\
c_\eta^0 &= -\frac{Z_i}{p}(F - 2\epsilon C)\,.
\end{aligned}
\tag{3.29}
$$

The constants A, B, C, D, E, F and p are given by the values of the functions (2.10) and (2.11) at $Z = Z_i = Z_0$.

The expression in the natural coordinates for positions are the same as in (3.19) and for velocities as in (3.20); however, the coefficients are now of the form

$$
\begin{aligned}
a_x^0 &= -2\frac{\mathrm{Re}Z_i}{p}\,\mathrm{Re}(F - 2\epsilon C), \\
b_x^0 &= -2\frac{\mathrm{Re}Z_i}{p}\,\mathrm{Im}(F - 2\epsilon C), \\
c_x^0 &= \frac{\mathrm{Re}Z_i}{p}\,[E - D + 2\epsilon(A - B)], \\
d_x^0 &= \frac{\mathrm{Re}Z_i}{p}\,[E + D - 2\epsilon(A + B)], \\
a_y^0 &= -2\frac{\mathrm{Im}Z_i}{p}\,\mathrm{Re}(F - 2\epsilon C), \\
b_y^0 &= -2\frac{\mathrm{Im}Z_i}{p}\,\mathrm{Im}(F - 2\epsilon C), \\
c_y^0 &= \frac{\mathrm{Im}Z_i}{p}\,[E - D + 2\epsilon(A - B)], \\
d_y^0 &= \frac{\mathrm{Im}Z_i}{p}\,[E + D - 2\epsilon(A + B)],
\end{aligned}
\tag{3.30}
$$

$$
\begin{aligned}
a^0_z &= \frac{|Z_i|^2-1}{p}\,\mathrm{Re}(F-2\epsilon C)+(1-\epsilon)\,\mathrm{Re}C,\\
b^0_z &= \frac{|Z_i|^2-1}{p}\,\mathrm{Im}(F-2\epsilon C)+(1-\epsilon)\,\mathrm{Im}C,\\
c^0_z &= \frac{|Z_i|^2-1}{2p}\,[-E+D-2\epsilon(A-B)]+\tfrac{1}{2}(1-\epsilon)(A-B),\\
d^0_z &= \frac{|Z_i|^2-1}{2p}\,[-E-D+2\epsilon(A+B)]-\tfrac{1}{2}(1-\epsilon)(A+B),\\
a^0_t &= -\frac{|Z_i|^2+1}{p}\,\mathrm{Re}(F-2\epsilon C)-(1+\epsilon)\,\mathrm{Re}C,\\
b^0_t &= -\frac{|Z_i|^2+1}{p}\,\mathrm{Im}(F-2\epsilon C)-(1+\epsilon)\,\mathrm{Im}C,\\
c^0_t &= \frac{|Z_i|^2+1}{2p}\,[E-D+2\epsilon(A-B)]-\tfrac{1}{2}(1+\epsilon)(A-B),\\
d^0_t &= \frac{|Z_i|^2+1}{2p}\,[E+D-2\epsilon(A+B)]+\tfrac{1}{2}(1+\epsilon)(A+B).
\end{aligned}
$$

From (3.13) we can extract a complex constraint for the velocities. From it we can see which geodesics are included in our special family. We get

$$
\dot\eta^+_i\bar C_{,\bar Z}+\dot{\bar\eta}^+_i C_{,\bar Z}-\dot{\mathrm{U}}^+_i A_{,\bar Z}-\dot V^+_i B_{,\bar Z}=0\,. \tag{3.31}
$$

We may express two real components of the velocity in terms of the remaining two, namely

$$
\begin{aligned}
\dot y^+_i &= \frac{\dot x^+_i[(B-A)\,\mathrm{Im}F-(E-D)\,\mathrm{Im}C]+2\dot z^+_i(\mathrm{Re}C\,\mathrm{Im}F-\mathrm{Im}C\,\mathrm{Re}F)}{(B-A)\,\mathrm{Re}F-(E-D)\,\mathrm{Re}C}\\
\dot t^+_i &= \frac{\dot x^+_i(BD-AE)-\dot z^+_i[(B+A)\,\mathrm{Re}F-(E+D)\,\mathrm{Re}C]}{(B-A)\,\mathrm{Re}F-(E-D)\,\mathrm{Re}C}\,.
\end{aligned} \tag{3.32}
$$

Substituting these two relations and the coefficients (3.30) into (3.20), and using equations (3.20), which relate the interaction positions, we finally obtain

$$
\begin{aligned}
\dot x^-_i &= x^-_i\frac{(E-D)\,\dot x^+_i+2\mathrm{Re}F\,\dot z^+_i}{(E-D)\,x^+_i+2\mathrm{Re}F\,z^+_i},\\
\dot y^-_i &= y^-_i\frac{(E-D)\,\dot x^+_i+2\mathrm{Re}F\,\dot z^+_i}{(E-D)\,x^+_i+2\mathrm{Re}F\,z^+_i},\\
\dot z^-_i &= \frac{z^-_i[(E-D)\,\dot x^+_i+2\mathrm{Re}F\,\dot z^+_i]-(1-\epsilon)(z^+_i\dot x^+_i-\dot z^+_i x^+_i)}{(E-D)\,x^+_i+2\mathrm{Re}F\,z^+_i}\,,\\
\dot t^-_i &= \frac{t^-_i[(E-D)\,\dot x^+_i+2\mathrm{Re}F\,\dot z^+_i]+(1+\epsilon)(z^+_i\dot x^+_i-\dot z^+_i x^+_i)}{(E-D)\,x^+_i+2\mathrm{Re}F\,z^+_i}.
\end{aligned} \tag{3.33}
$$

e should emphasize that the construction above, as we have done, overlooks the fact that we began with our initial data outside the impulse, which is Minkowski only locally. Because of the form of the complex function h, there are topological defects outside the null cone. For a better physical approach to the derivation, we could swap the coordinate systems, thus having the topological defects inside the null cone. As another option, we can start with the initial position in the null cone and then backward the time and thus cross the impulse from inside out. However, we would arrive at the same result [30].

4. Geodesics in spacetime with one cosmic string

We are going to now resort to a specific expanding impulsive spacetime with a single cosmic string. It is generated by a snap of such a cosmic string, whose remnants are two semi-infinite strings located along the z-axis outside the impulsive wave. The warp function makes a conical singularity $h(Z) = Z^{1-\delta}$, where δ is a real positive constant, and $\delta < 1$. The resulting function in the metric (2.14)

$$H(Z) = \frac{\frac{1}{2}\delta(1-\frac{1}{2}\delta)}{Z^2}\,. \tag{4.1}$$

The parameter δ characterizes the deficit angle $2\pi\delta$ of the snapped string localized outside the impulse along the z-axis [29].

4.1 General geodesics behaviour

It is now straightforward to compute the coefficients in (2.10), which are [29]

$$\begin{aligned}
A &= \frac{|Z|^{\delta}}{(1-\delta)p}\,, \qquad B = \frac{|Z|^{2-\delta}}{(1-\delta)p}\,, \qquad C = \frac{Z^{1-\delta}|Z|^{\delta}}{(1-\delta)p}\,,\\
D &= \frac{|Z|^{\delta-2}}{1-\delta}\left[(\tfrac{1}{2}\delta)^2 + (1-\tfrac{1}{2}\delta)^2\epsilon|Z|^2\right]\,,\\
E &= \frac{|Z|^{-\delta}}{1-\delta}\left[(1-\tfrac{1}{2}\delta)^2 + (\tfrac{1}{2}\delta)^2\epsilon|Z|^2\right]\,,\\
F &= \frac{Z^{1-\delta}|Z|^{\delta-2}\frac{1}{2}\delta(1-\frac{1}{2}\delta)p}{1-\delta}\,,\\
A_{,Z} &= \frac{|Z|^{\delta}[\frac{1}{2}\delta - (1-\frac{1}{2}\delta)\epsilon|Z|^2]}{(1-\delta)p^2 Z}\,,\\
B_{,Z} &= \frac{|Z|^{2-\delta}[(1-\frac{1}{2}\delta) - \frac{1}{2}\delta\epsilon|Z|^2]}{(1-\delta)p^2 Z}\,,\\
C_{,Z} &= \left(\frac{\bar{Z}}{Z}\right)^{\delta/2}\frac{(1-\frac{1}{2}\delta) - \frac{1}{2}\delta\epsilon|Z|^2}{(1-\delta)p^2}\,,\\
C_{,\bar{Z}} &= \left(\frac{\bar{Z}}{Z}\right)^{\delta/2-1}\frac{\frac{1}{2}\delta - (1-\frac{1}{2}\delta)\epsilon|Z|^2}{(1-\delta)p^2}\,.
\end{aligned} \tag{4.2}$$

For an easier illustration, it is convenient to introduce a new set of spatial parameters [30]. Specifically, in the (x,z) section we define

$$\tan\alpha^{\pm} = \frac{x_i^{\pm}}{z_i^{\pm}}\,, \qquad \tan\beta^{\pm} = \frac{\dot{x}_i^{\pm}}{\dot{z}_i^{\pm}}\,, \tag{4.3}$$

while in the perpendicular (y,z) section we define

$$\tan\gamma^{\pm} = \frac{y_i^{\pm}}{z_i^{\pm}}\,, \qquad \tan\delta^{\pm} = \frac{\dot{y}_i^{\pm}}{\dot{z}_i^{\pm}}\,. \tag{4.4}$$

We can now substitute this into (3.19) and (3.20) to obtain the following expressions, which identify the positions

$$\tan\alpha^- = \frac{(|h|^2-1)\,\mathrm{Re}\,Z_i}{(|Z_i|^2-1)\mathrm{Re}\,h}\tan\alpha^+\,,$$
$$\tan\gamma^- = \frac{(|h|^2-1)\,\mathrm{Im}\,Z_i}{(|Z_i|^2-1)\mathrm{Im}\,h}\tan\gamma^+\,, \tag{4.5}$$

and inclinations of the velocity vector,

$$\tan\beta^- = \frac{v_z^+(a_x\tan\beta^+ + b_x\tan\delta^+ + c_x)+d_x}{v_z^+(a_z\tan\beta^+ + b_z\tan\delta^+ + c_z)+d_z}\,,$$
$$\tan\delta^- = \frac{v_z^+(a_y\tan\beta^+ + b_y\tan\delta^+ + c_y)+d_y}{v_z^+(a_z\tan\beta^+ + b_z\tan\delta^+ + c_z)+d_z}\,, \tag{4.6}$$

on both sides of the impulse. These relations are general for any geodesics.

We will now follow the approach of [30] and express these relations in the case of our spacetime. We evaluate the equations (3.19)–(3.21). In particular, equations for positions (in the natural conformally flat background coordinates on both sides of the impulse) become

$$\begin{aligned}
x_i^- &= (1-\delta)\,|Z_i|^{-\delta}\frac{Z_i+\bar Z_i}{Z_i^{1-\delta}+\bar Z_i^{1-\delta}}\,x_i^+,\\
y_i^- &= (1-\delta)\,|Z_i|^{-\delta}\frac{Z_i-\bar Z_i}{Z_i^{1-\delta}-\bar Z_i^{1-\delta}}\,y_i^+,\\
z_i^- &= (1-\delta)\,\frac{|Z_i|-|Z_i|^{-1}}{|Z_i|^{1-\delta}-|Z_i|^{\delta-1}}\,z_i^+,\\
t_i^- &= (1-\delta)\,\frac{|Z_i|+|Z_i|^{-1}}{|Z_i|^{1-\delta}+|Z_i|^{\delta-1}}\,t_i^+.
\end{aligned} \tag{4.7}$$

Similarly, it is straightforward to evaluate the specific form of the coefficients which relate to the velocities, namely

$$\begin{aligned}
a_x &= \frac{|Z_i|^\delta}{2(1-\delta)}\Big[(1-\tfrac12\delta)^2(Z_i^{-\delta}+\bar Z_i^{-\delta})+\tfrac14\delta^2|Z_i|^{-2}(Z_i^{2-\delta}+\bar Z_i^{2-\delta})\Big],\\
b_x &= \frac{|Z_i|^\delta}{2\mathrm{i}(1-\delta)}\Big[(1-\tfrac12\delta)^2(Z_i^{-\delta}-\bar Z_i^{-\delta})+\tfrac14\delta^2|Z_i|^{-2}(Z_i^{2-\delta}-\bar Z_i^{2-\delta})\Big],\\
c_x &= \frac{\delta(1-\frac12\delta)}{4(1-\delta)}|Z_i|^\delta\Big[(Z_i^{-1}+\bar Z_i^{-1})-|Z_i|^{-2\delta}(Z_i+\bar Z_i)\Big],\\
d_x &= -\frac{\delta(1-\frac12\delta)}{4(1-\delta)}|Z_i|^\delta\Big[(Z_i^{-1}+\bar Z_i^{-1})+|Z_i|^{-2\delta}(Z_i+\bar Z_i)\Big],
\end{aligned} \tag{4.8}$$

$$\begin{aligned}
a_y &= \frac{\mathrm{i}\,|Z_i|^\delta}{2(1-\delta)}\Big[(1-\tfrac12\delta)^2(Z_i^{-\delta}-\bar Z_i^{-\delta})-\tfrac14\delta^2|Z_i|^{-2}(Z_i^{2-\delta}-\bar Z_i^{2-\delta})\Big],\\
b_y &= \frac{|Z_i|^\delta}{2(1-\delta)}\Big[(1-\tfrac12\delta)^2(Z_i^{-\delta}+\bar Z_i^{-\delta})-\tfrac14\delta^2|Z_i|^{-2}(Z_i^{2-\delta}+\bar Z_i^{2-\delta})\Big],\\
c_y &= \frac{\mathrm{i}\delta(1-\frac12\delta)}{4(1-\delta)}|Z_i|^\delta\Big[(Z_i^{-1}-\bar Z_i^{-1})+|Z_i|^{-2\delta}(Z_i-\bar Z_i)\Big],\\
d_y &= \frac{\delta(1-\frac12\delta)}{4\mathrm{i}(1-\delta)}|Z_i|^\delta\Big[(Z_i^{-1}-\bar Z_i^{-1})-|Z_i|^{-2\delta}(Z_i-\bar Z_i)\Big],
\end{aligned} \tag{4.9}$$

$$
\begin{aligned}
a_z &= \frac{\delta(1-\frac{1}{2}\delta)}{4(1-\delta)}|Z_i|^{\delta}\Big[(Z_i^{1-\delta}+\bar{Z}_i^{1-\delta})-|Z_i|^{-2}(Z_i^{1-\delta}+\bar{Z}_i^{1-\delta})\Big],\\
b_z &= \frac{\delta(1-\frac{1}{2}\delta)}{4\mathrm{i}(1-\delta)}|Z_i|^{\delta}\Big[(Z_i^{1-\delta}-\bar{Z}_i^{1-\delta})-|Z_i|^{-2}(Z_i^{1-\delta}-\bar{Z}_i^{1-\delta})\Big],\\
c_z &= \frac{1}{2(1-\delta)}\Big[(1-\tfrac{1}{2}\delta)^2(|Z_i|^{\delta}+|Z_i|^{-\delta})-\tfrac{1}{4}\delta^2(|Z_i|^{2-\delta}+|Z_i|^{\delta-2})\Big],\\
d_z &= \frac{-1}{2(1-\delta)}\Big[(1-\tfrac{1}{2}\delta)^2(|Z_i|^{\delta}-|Z_i|^{-\delta})+\tfrac{1}{4}\delta^2(|Z_i|^{2-\delta}-|Z_i|^{\delta-2})\Big],
\end{aligned}
\tag{4.10}
$$

$$
\begin{aligned}
a_t &= -\frac{\delta(1-\frac{1}{2}\delta)}{4(1-\delta)}|Z_i|^{\delta}\Big[(Z_i^{1-\delta}+\bar{Z}_i^{1-\delta})+|Z_i|^{-2}(Z_i^{1-\delta}+\bar{Z}_i^{1-\delta})\Big],\\
b_t &= \frac{\mathrm{i}\delta(1-\frac{1}{2}\delta)}{4(1-\delta)}|Z_i|^{\delta}\Big[(Z_i^{1-\delta}-\bar{Z}_i^{1-\delta})+|Z_i|^{-2}(Z_i^{1-\delta}-\bar{Z}_i^{1-\delta})\Big],\\
c_t &= \frac{-1}{2(1-\delta)}\Big[(1-\tfrac{1}{2}\delta)^2(|Z_i|^{\delta}-|Z_i|^{-\delta})-\tfrac{1}{4}\delta^2(|Z_i|^{2-\delta}-|Z_i|^{\delta-2})\Big],\\
d_t &= \frac{1}{2(1-\delta)}\Big[(1-\tfrac{1}{2}\delta)^2(|Z_i|^{\delta}+|Z_i|^{-\delta})+\tfrac{1}{4}\delta^2(|Z_i|^{2-\delta}+|Z_i|^{\delta-2})\Big].
\end{aligned}
\tag{4.11}
$$

We can see from the structure of the coefficients that it is convenient to parameterize the complex coordinate Z_i using the polar form

$$
Z_i \equiv R\, e^{\mathrm{i}\,\Phi}\,, \tag{4.12}
$$

where $R = |Z_i|$ and Φ are constants representing its modulus and phase, respectively [30]. By definition, the relation to natural coordinates is

$$
\begin{aligned}
R &= \left(\frac{(x_i^+)^2+(y_i^+)^2}{(t_i^+ + z_i^+)^2}\right)^{\frac{1}{2(1-\delta)}} = \left(\frac{t_i^+ - z_i^+}{t_i^+ + z_i^+}\right)^{\frac{1}{2(1-\delta)}}\,,\\
\tan\big((1-\delta)\Phi\big) &= \frac{y_i^+}{x_i^+}\,.
\end{aligned}
\tag{4.13}
$$

We can further define a logarithm of R as

$$
r \equiv \log R = \frac{1}{2(1-\delta)}\log\left(\frac{t_i^+ - z_i^+}{t_i^+ + z_i^+}\right). \tag{4.14}
$$

For the sake of simplicity, we are going to take geodesics which are at rest in front of the impulse (in the region with the conical singularity), i.e., $\dot{x}^+ = \dot{y}^+ = \dot{z}^+ = 0$. This significantly reduces the equations (3.20) to

$$
\dot{x}_i^- = d_x\,\dot{t}_i^+\,, \qquad \dot{y}_i^- = d_y\,\dot{t}_i^+\,, \qquad \dot{z}_i^- = d_z\,\dot{t}_i^+\,, \qquad \dot{t}_i^- = d_t\,\dot{t}_i^+\,. \tag{4.15}
$$

Using the new parameterization, we get the refraction formulae for the angles

$$
\begin{aligned}
\tan\alpha^- &= \frac{\sinh\big((1-\delta)r\big)}{\sinh r}\,\frac{\cos\Phi}{\cos\big((1-\delta)\Phi\big)}\,\tan\alpha^+,\\
\tan\beta^- &= \frac{\delta(1-\frac{1}{2}\delta)\cosh\big((1-\delta)r\big)\cos\Phi}{(1-\frac{1}{2}\delta)^2\sinh(\delta r)+\frac{1}{4}\delta^2\sinh\big((2-\delta)r\big)},
\end{aligned}
\tag{4.16}
$$

and

$$\begin{aligned}\tan\gamma^- &= \frac{\sinh\big((1-\delta)r\big)}{\sinh r}\,\frac{\sin\Phi}{\sin\big((1-\delta)\Phi\big)}\,\tan\gamma^+, \\ \tan\delta^- &= \frac{\delta(1-\frac{1}{2}\delta)\cosh\big((1-\delta)r\big)\sin\Phi}{(1-\frac{1}{2}\delta)^2\sinh(\delta r)+\frac{1}{4}\delta^2\sinh\big((2-\delta)r\big)}.\end{aligned} \tag{4.17}$$

Due to axial symmetry along the z-axis, we can simplify our analysis to the(x^+, z^+) plane, thus assuming $y^+ = 0$. From this assumption and the fact that we take static particles in front of the impulse, we see that $\gamma^\pm = 0 = \delta^\pm$, further reducing our refraction formulae to

$$\begin{aligned}\tan\alpha^- &= \frac{\sinh\big((1-\delta)r\big)}{\sinh r}\,\tan\alpha^+, \\ \tan\beta^- &= \frac{\delta(1-\frac{1}{2}\delta)\cosh\big((1-\delta)r\big)}{(1-\frac{1}{2}\delta)^2\sinh(\delta r)+\frac{1}{4}\delta^2\sinh\big((2-\delta)r\big)},\end{aligned} \tag{4.18}$$

where r is simplified to $r = \frac{1}{1-\delta}\log\left(\tan\frac{\alpha^+}{2}\right)$, see [30].

It is now possible to visualize the impact of the impulse generated by a snapped cosmic string on a ring of test particles by plotting the corresponding graphs. Firstly, we will reproduce the graphs made by Podolský and Švarc in [30], so we can then compare them with those for the privileged geodesics $Z = \text{const}$.

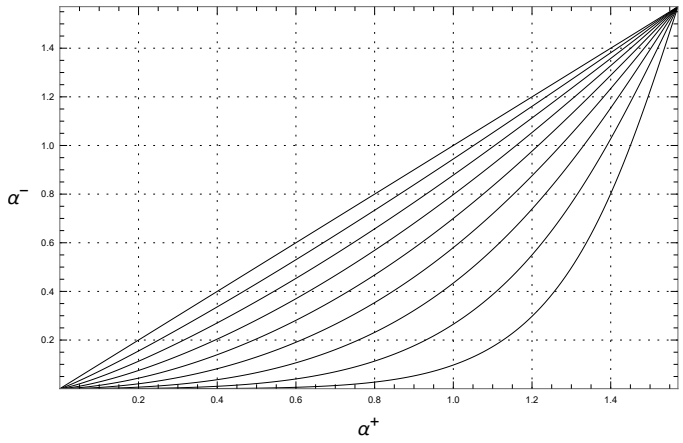

Figure 4.1: The function $\alpha^-(\alpha^+)$ determines the dependence of the position behind the impulse on the particle position in front of the impulse. The curves plotted correspond to $\delta = 0.1, 0.2, \ldots, 0.8$.

In figures 4.1 and 4.2, we present the functions $\alpha^-(\alpha^+)$ and $\beta^-(\alpha^+)$, respectively, as described by equation (4.18) for several discrete values of the parameter δ. The angle α^+ represents the position of a particle in the ring ahead of the impulse, while α^- and β^- indicate its position and velocity vector inclination behind the impulse, respectively.

By combining these two relations, we plot the motion of the (initially static) ring caused by the impulse in figure 4.3. It is evident that the particles are displaced towards the string, and their velocity directions are aligned "along" the string. Particles located close to the string ahead of the impulse are accelerated

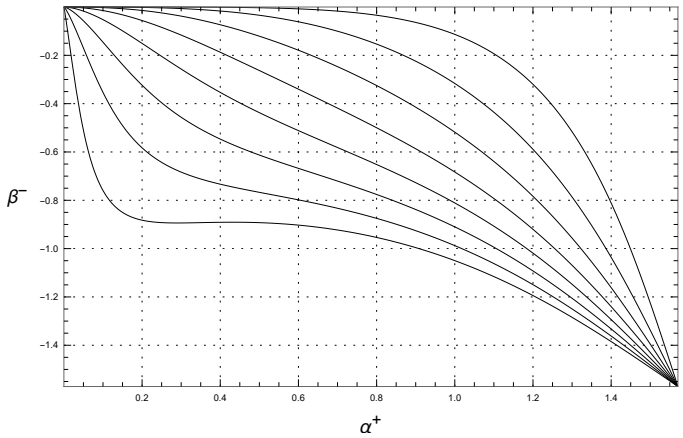

Figure 4.2: The function $\beta^-(\alpha^+)$ determines the dependence of the velocity vector inclination behind the impulse on the particle position in front of the impulse. The curves plotted correspond to $\delta = 0.1,\, 0.2, \ldots,\, 0.8$.

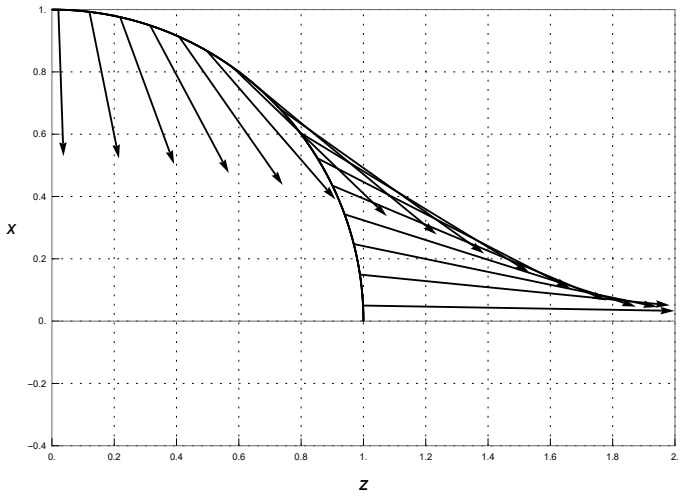

Figure 4.3: The effect of the impulse with $\delta = 0.4$ on a semi-ring of static particles in front of the impulse in the (x, z) plane. The particles are shifted (not visualized) immediately in the direction of their velocity represented by the vectors (v_x^-, v_z^-).

to nearly the speed of light behind the impulse, being "dragged" along the string (except for those in the perpendicular plane $z = 0$ corresponding to $\alpha_+ = \frac{\pi}{2}$).

To see this more clearly we plot the velocity components with respect to the Minkowski frame behind the impulse. These are given by

$$(v_x^-, v_y^-, v_z^-) = \left(\frac{\dot{x}_i^-}{\dot{t}_i^-}, \frac{\dot{y}_i^-}{\dot{t}_i^-}, \frac{\dot{z}_i^-}{\dot{t}_i^-} \right). \tag{4.19}$$

In figure 4.4, we plot the magnitude $v^- = \sqrt{(v_x^-)^2 + (v_z^-)^2}$ of the resulting velocity vector as a function of α_+ for several values of the parameter δ. For small values of the angle α_+, the speed approaches that of light, i.e., $v^- \to 1$. The components $v_x^- = \left(\frac{\dot{x}_i^-}{\dot{t}_i^-}\right)$ and $v_z^- = \left(\frac{\dot{z}_i^-}{\dot{t}_i^-}\right)$ are separately illustrated in figure 4.5.

Finally, in figure 4.6 we visualize the deformation of the ring of test particles, initially at rest, as it evolves with time. It can be concluded that the circle (which may be considered as a (x, z) section through a sphere) is deformed by the

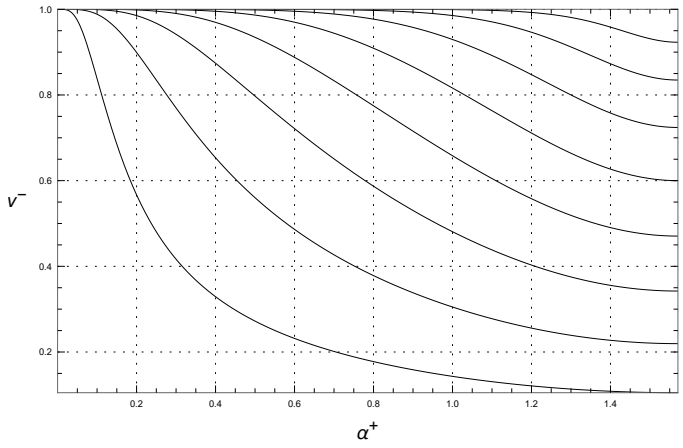

Figure 4.4: The magnitude of the velocity v^- behind the impulse with respect to the initial position α^+. The curves plotted correspond to $\delta = 0.1, 0.2, \ldots, 0.8$.

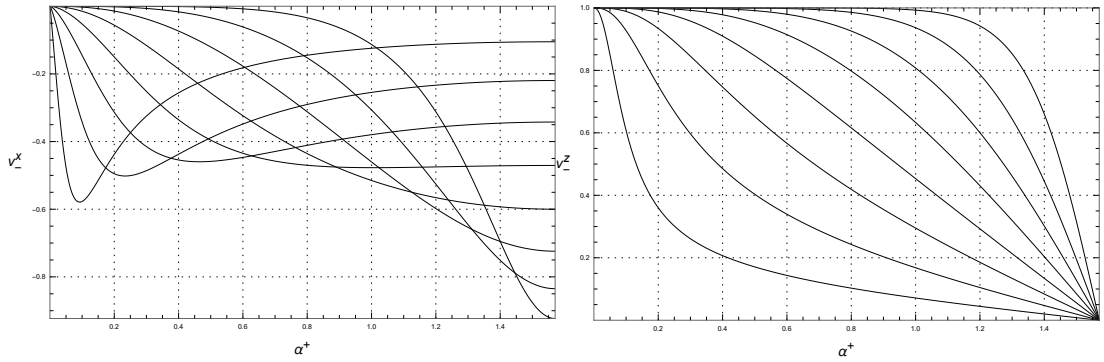

Figure 4.5: The components v_x^- and v_z^- of the velocity behind the impulse with respect to the initial position α^+. The curves plotted correspond to $\delta = 0.1, 0.2, \ldots, 0.8$.

gravitational impulse into an axially symmetric pinched surface, elongated and expanding along the moving strings in the positive z-direction. Also, the particles which initially started at $x > 0$ have $v_x^- < 0$, while those with $x < 0$ have $v_x^- > 0$. This explicitly demonstrates the "dragging" effect in such spacetimes caused by the moving strings and the corresponding impulse. With a growing value of the parameter δ, the deformation in the z-direction is bigger [30].

4.2 Privileged geodesics behaviour

Firstly, we derive the refraction formulae following the approach of Podolský and Steinbauer [29]. Afterwards, we are going to produce graphs for this special family of geodesics with a focus on the null geodesics.

It is convenient to use the global axial symmetry of the solution [29, 30] corresponding to a coordinate freedom $Z \to Z \exp(\mathrm{i}\phi)$, where ϕ is a constant. Therefore, without loss of generality, we can assume $Z = Z_i = Z_0$ to be a *real*

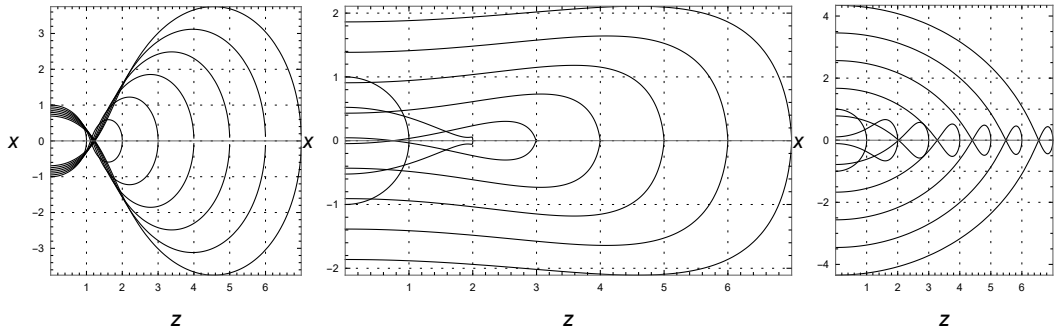

Figure 4.6: Time sequence showing the deformation of a ring of particles in the (x, z) plane. The curves plotted correspond to $\delta = 0.05,\ 0.35,\ 0.8$.

positive constant, in which case the coefficients (4.2) reduce to

$$\begin{aligned} A &= \frac{Z_0^{\delta}}{(1-\delta)p}\ , \qquad B = \frac{Z_0^{2-\delta}}{(1-\delta)p}\ , \qquad C = \frac{Z_0}{(1-\delta)p}\ , \\ D &= \frac{Z_0^{\delta-2}}{1-\delta}\left[(\tfrac{1}{2}\delta)^2 + (1-\tfrac{1}{2}\delta)^2\epsilon Z_0^2\right]\ , \\ E &= \frac{Z_0^{-\delta}}{1-\delta}\left[(1-\tfrac{1}{2}\delta)^2 + (\tfrac{1}{2}\delta)^2\epsilon Z_0^2\right]\ , \\ F &= \frac{\frac{1}{2}\delta(1-\frac{1}{2}\delta)p}{(1-\delta)Z_0}\ , \end{aligned} \tag{4.20}$$

where $p = 1 + \epsilon Z_0^2$.

However, to remain in our family of privileged geodesics, we now do not have the freedom to choose any initial data, i.e., "static" geodesics. We have to abide by the equations (3.31). In the previous section, by choosing such geodesics, we were able to get rid of any dependence on ϵ. Yet due to axial symmetry, we can still keep our analysis in the (x, z) plane. The refraction formulae now have the form

$$\begin{aligned} x_0^- &= (1-\delta)\, x_0\ , \\ y_0^- &= 0\ , \\ z_0^- &= \tfrac{1}{2}(1-\delta)\, x_0(Z_0 - Z_0^{-1})\ , \\ t_0^- &= \tfrac{1}{2}(1-\delta)\, x_0(Z_0 + Z_0^{-1})\ , \\ \dot{x}_0^- &= (1-\delta)\, x_0 \frac{(E-D)\,\dot{x}_0 - 2F\,\dot{z}_0}{(E-D)\,x_0 - 2F\,z_0}\ , \\ \dot{y}_0^- &= 0\ , \\ \dot{z}_0^- &= \frac{z_0^-\left[(E-D)\,\dot{x}_0 - 2F\,\dot{z}_0\right] - (1-\epsilon)(z_0\dot{x}_0 - x_0\dot{z}_0)}{(E-D)\,x_0 - 2F\,z_0}\ , \\ \dot{t}_0^- &= \frac{t_0^-\left[(E-D)\,\dot{x}_0 - 2F\,\dot{z}_0\right] - (1+\epsilon)(z_0\dot{x}_0 - x_0\dot{z}_0)}{(E-D)\,x_0 - 2F\,z_0}\ . \end{aligned} \tag{4.21}$$

Again, we use our parametrization through the angles $\alpha^{\pm}$ and $\beta^{\pm}$. Together with the constraint for velocities, we get one equation for all the four angles

$$\cot\beta^- - \cot\alpha^- = \mathcal{N}\left(\cot\beta^+ - \cot\alpha^+\right)\ , \tag{4.22}$$

where

$$\mathcal{N} = \mathcal{N}(\alpha^+, \beta^+) = \frac{1-\epsilon}{(1-\delta)(E-D) - (1-\delta)\,2F\cot\beta^+}\ . \tag{4.23}$$

This is the refraction formula for trajectories of free test particles that cross the spherical impulse. Several interesting observations can immediately be made.

For $\delta = 0$, representing a complete Minkowski space without the impulse and topological defects, we obtain $\alpha^- = \alpha^+$, $\mathcal{N} = 1$, and consequently $\beta^- = \beta^+$. Thus, there is no "shift" or "refraction", as expected.

For a general δ, it follows from (4.22) that if $\alpha^+ = \beta^+$, then $\alpha^- = \beta^-$. This means physically that the radial geodesics ("perpendicular" to the spherical impulse) remain radial even behind the impulse.

Moreover, it can be observed from (4.23) that the coefficient $\mathcal{N}$ identically vanishes for spacetimes with the parameter $\epsilon = 1$. Consequently, $\alpha^- = \beta^-$ indicates that the geodesics (3.8) are refracted by the impulse in such a way that their trajectories become radial. Thus these are either focused exactly towards the origin, $x = 0 = z$, or defocused directly away from it.

Exactly this behavior, for $\epsilon = 0$, is visualised in figures 4.7 and 4.8. The inclination angle behind the impulse β^- does not change for different inclination angles β^+ of the geodesics in front of the impulse. In the latter graph, we also perceive a jump in β^-. The relation between the position angles is not shown as it is the same as before, see 4.1.

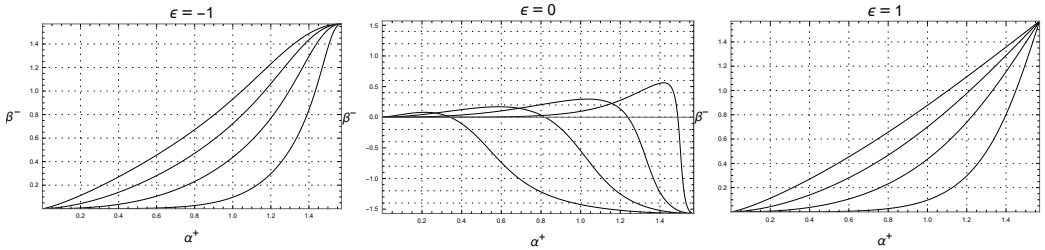

Figure 4.7: The function $\beta^-(\alpha^+)$ which determines the dependence of the velocity vector inclination behind the impulse on the particle position in front of the impulse and the initial velocity angle $\beta^+ = \frac{\pi}{2}$. The curves plotted correspond to $\delta = 0.2,\ 0.4, \ldots,\ 0.8$.

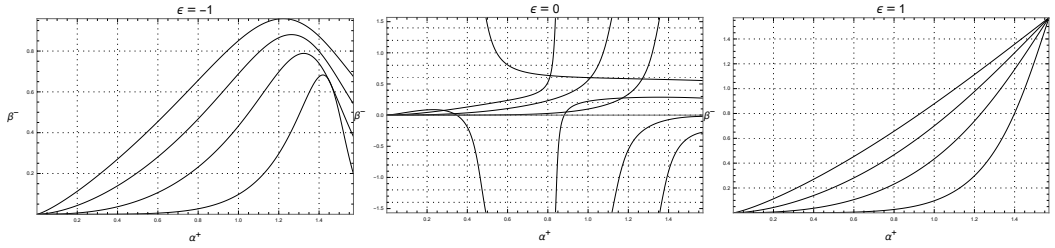

Figure 4.8: The function $\beta^-(\alpha^+)$ which determines the dependence of the velocity vector inclination behind the impulse on the particle position in front of the impulse and the initial velocity angle $\beta^+ = \frac{\pi}{4}$. The curves plotted correspond to $\delta = 0.2,\ 0.4, \ldots,\ 0.8$.

By combining these two equations, we are able to plot the motion of particles crossing the impulse in figure 4.9. Each test particle follows in the region $U > 0$

a trajectory with the inclination angle β^+ until it reaches the spherical impulse at the point represented by α^+. The impulse influences the particle in such a way that it emerges in the region $U < 0$ shifted to a new point given by α^-, and (4.22) continues to move uniformly along the straight trajectory with inclination β^-. This illustration however provides only the directions, not the magnitudes. For that see [29].

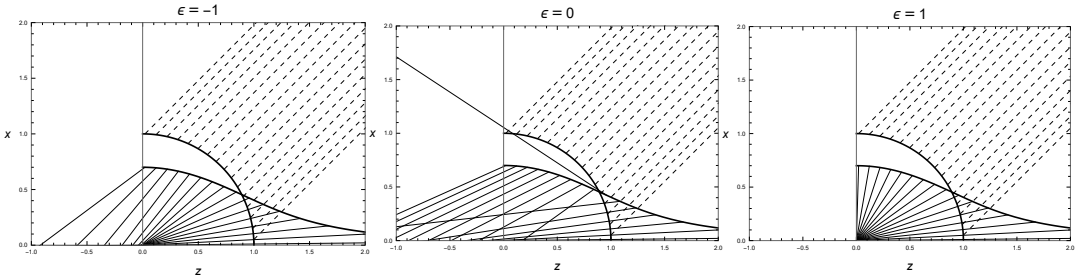

Figure 4.9: The trajectories of geodesics from the privileged family. The dotted lines indicate the trajectory in front of the impulse for $\beta^+ = \frac{\pi}{4}$ hitting the impulse indicated as a semi-circle. Their position is shifted, and their velocity vector changes direction. The trajectories plotted are with $\delta = 0.3$.

To investigate the magnitude of velocities we plot the velocity components (4.19). In figures 4.10 and 4.11, we show the components as a function of α^+ for several values of δ, and $\beta^+ = \frac{\pi}{4}$. We then show the resulting magnitude v^- in figure 4.12. As can be seen with the components and the magnitude, it diverges for some values of α^+ corresponding to the tachyons. The placement of these points is determined by a complex dependency on α^+, β^+, ϵ and δ. We can also see that for α^+ small enough, the speed approaches that of light, i.e., $v^- \to 1$.

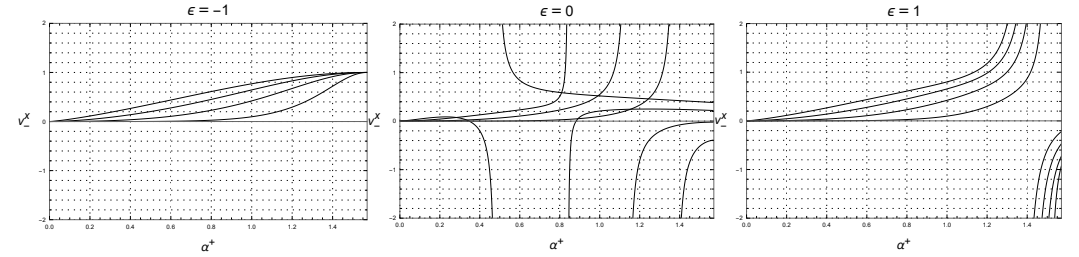

Figure 4.10: The component v_x^- of the velocity behind the impulse with respect to initial position α^+, and for $\beta^+ = \frac{\pi}{4}$. The curves plotted correspond to $\delta = 0.2, 0.4, \ldots, 0.8$.

Similar to the case with general geodesics, we examine how test particles are deformed upon encountering the impulse simultaneously. This is visualized in figure 4.13. Yet this is done only for $\epsilon = 1$ as the divergence in the velocities proves rather tricky to visualize for the other values. Here we see, correspondingly to the velocity magnitude, that for a certain value of α, the particles are refracted to infinity, and for even higher values close to $\frac{\pi}{2}$, they retract towards the string.

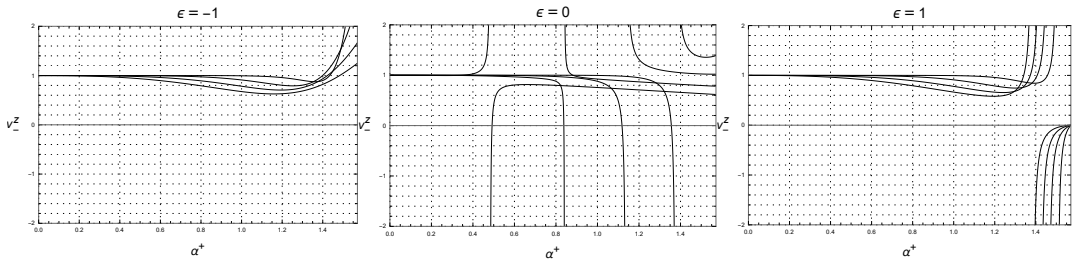

Figure 4.11: The component v_z^- of the velocity behind the impulse with respect to initial position α^+, and for $\beta^+ = \frac{\pi}{4}$. The curves plotted correspond to $\delta = 0.2, 0.4, \ldots, 0.8$.

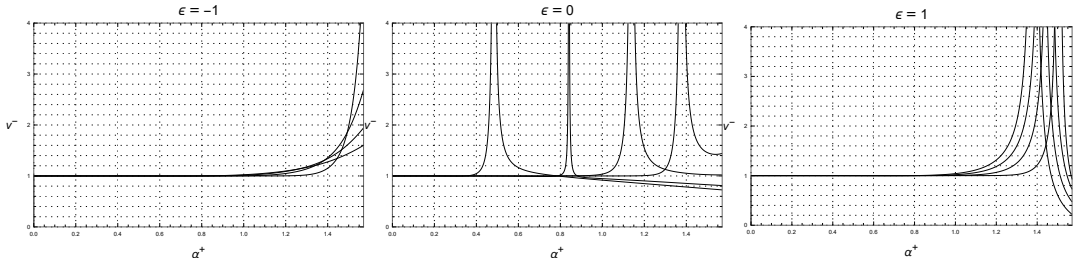

Figure 4.12: The magnitude of the velocity v^- behind the impulse with respect to initial position α^+, and for $\beta^+ = \frac{\pi}{4}$. The curves plotted correspond to $\delta = 0.2, 0.4, \ldots, 0.8$.

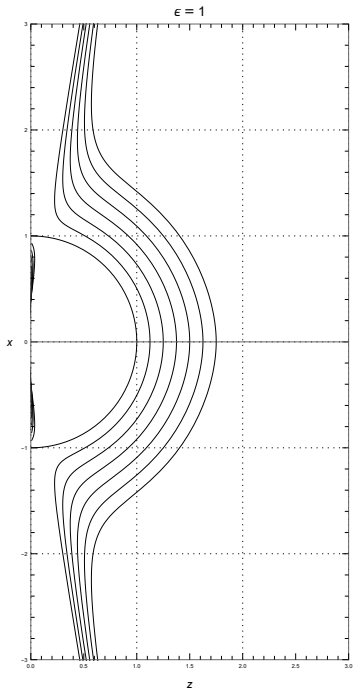

Figure 4.13: Time sequence showing the deformation of a ray of particles, with inclination angle $\beta^+ = \frac{\pi}{4}$ from the z axis, in the (x, z) plane. The curves plotted correspond to $\delta = 0.3$.

In particular, we would like to look at the null geodesics from the privileged family which could be further used as new coordinate lines. This should be an analogy with the nonexpanding case, where to derive the transformation formulae (see Chapter 3), we used null geodesics in front of the impulse. When $v_- =$

$\sqrt{(v_x^-)^2 + (v_z^-)^2}$ is equal to 1, we have a null geodesics. Substituting into this constraint, we get a quadratic equation for $\cot\beta^+$ which can be solved. In the range $\alpha^+ \in (0, \frac{\pi}{2}]$ there are always two real roots, namely

$$\begin{aligned} &1. \quad \beta^+_{null} = \alpha^+ \ , \\ &2. \quad \cot\beta^+_{null} = \frac{\epsilon\cot\alpha^+ - \frac{1}{2}(Z_0^{-1} + \epsilon Z_0)(1-\delta)(E-D)}{\epsilon - \frac{1}{2}(Z_0^{-1} + \epsilon Z_0)(1-\delta)\,2F} \ . \end{aligned} \tag{4.24}$$

The first solution gives us geodesics that move radially outside the impulse. These are exactly those null geodesics that generate the spherical impulse itself. The second equation gives us a more interesting case.

Now, having the refraction formulae for the privileged geodesics, we intend to illustrate these solutions and, if possible, compare them with the graphs for general geodesics. We will proceed in the same manner as before. Firstly, the dependence of the position behind the impulse is the same as for general geodesics. However, we now have a formula for β^+. This is illustrated in figure 4.14. The geodesics close to the z-axis move parallel to the impulse in front of the string, this is the strongest in the case for $\epsilon = 1$, and for $\epsilon = 0$ we see a jump in the angle. This is delicately illustrated in [29], where each case is thoroughly analyzed.

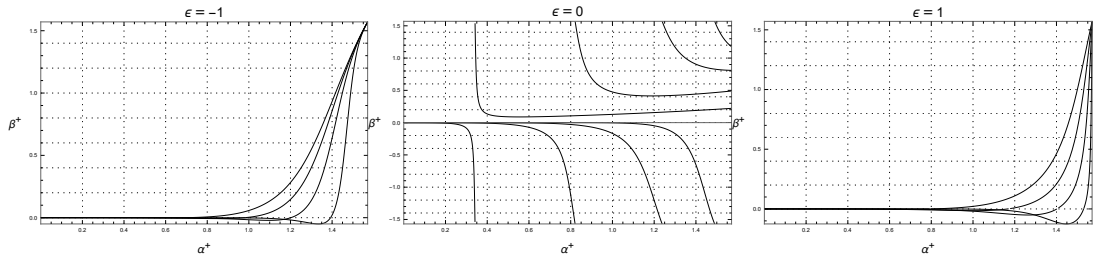

Figure 4.14: For null geodesics from the privileged family, the function $\beta^+(\alpha^+)$ determines the dependence of the velocity vector inclination in front of the impulse on the particle position in front of the impulse via (4.24). The curves plotted correspond to $\delta = 0.2, 0.4, \ldots, 0.8$.

We now look at the inclination angle behind the impulse β^-, see figure 4.15. As implied by (4.22) for the case $\epsilon = 1$, it is the same as for other privileged geodesics. Interestingly for $\epsilon = 0$, all the geodesics become parallel to the string.

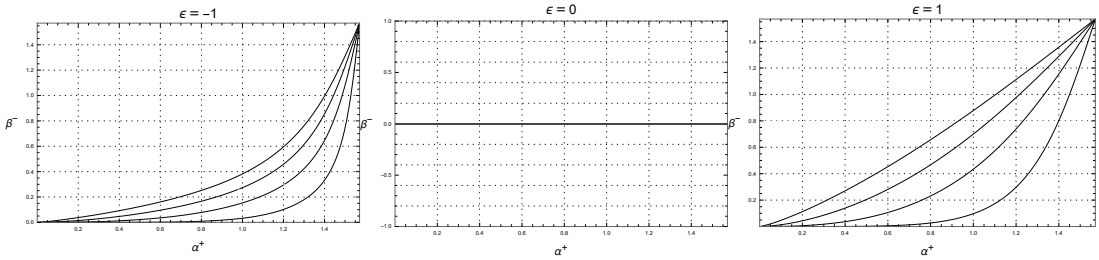

Figure 4.15: The function $\beta^-(\alpha^+)$ determines the dependence of the velocity vector inclination behind the impulse on the particle position in front of the impulse for null geodesics from the privileged family. The curves plotted correspond to $\delta = 0.2,\ 0.4, \ldots,\ 0.8$..

Combining these two relations, we plot the motion of null particles crossing the impulse in figure 4.9. Again, each particle follows, in the region $U > 0$, a

trajectory with the inclination angle β^+ until it reaches the spherical impulse at the point represented by α^+. The impulse shifts the particles in the region $U < 0$ to a new point given by α^- and (4.22), then the particles continue to move uniformly along the straight trajectory with inclination β^-.

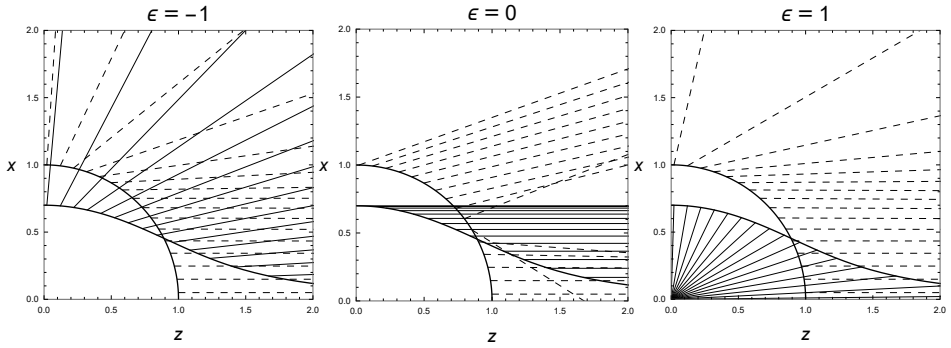

Figure 4.16: The trajectories of *null* geodesics from the privileged family. The dotted lines indicate the trajectory in front of the impulse hitting the impulse indicated as a semi-circle. Their position is shifted, and the velocity vector changes direction. The trajectories plotted are for $\delta = 0.3$.

The magnitudes of the velocity are now set to be $v^- = 1$. For $\epsilon = 0$ we have $v_x^- = 0$, corresponding to the fact that all the geodesics behind the impulse are parallel to the string. We show the components for the case $\epsilon = 1$, see figure 4.17. This corresponds to the fact, that the geodesics behind the impulse, in this case, must be radial.

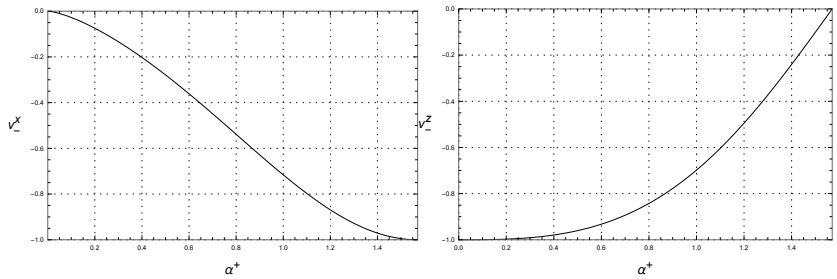

Figure 4.17: Components of velocity with respect to α^+. The curve plottes correspond to $\delta = 0.3$ and $\epsilon = 1$.

Finally, we illustrate the evolution of geodesics behind the impulse for different times in figure 4.18. It is done in the natural coordinates in front of the impulse, to better see the influence of the impulse. As the coordinate time behind the impulse t^- is defined by (4.21), the lines in 4.17 are not equidistant, as they are shown in the coordinate system in front of the impulse t^+. For $\epsilon = 0$, we see that the particles are moving along the impulse in the direction of the snapped string [30].

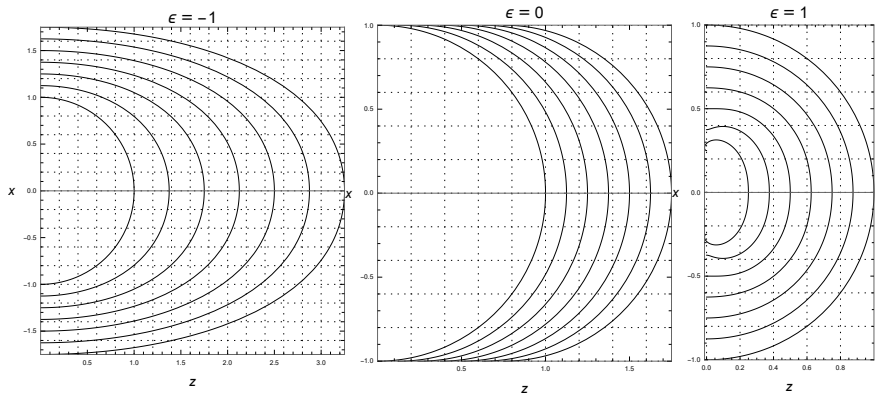

Figure 4.18: Time sequence showing the deformation of a ray of null particles in the (x, z) plane. The curves plotted correspond to $\delta = 0.3$.

Description of the privileged $Z = \text{const}$ class of null geodesics could be important in understanding the geometry of transformation that relates distributional and continuous coordinate systems. However, this task will be postponed for further research.

Conclusion

This thesis has provided a detailed summary of exact solutions to Einstein's field equations representing impulsive gravitational waves propagating in background spacetimes of constant curvature, i.e., in Minkowski, de Sitter, and anti-de Sitter spacetimes. We have specifically focused on the continuous and distributional parameterizations of these low regularity spacetimes in both cases of nonexpanding and expanding impulses, respectively, as well as on related descriptions of geodesics crossing the impulse.

Using the cut-and-paste techniques and the limits of sandwich wave solutions, we introduced the continuous and distributional forms of the metric for both cases on a heuristic level. Moreover, we have reviewed the derivation of a continuous coordinate system for the nonexpanding impulse with vanishing cosmological constant to motivate the rigorous mathematical framework necessary for understanding these phenomena and the importance of geodesics in description of these spacetimes. Since the analogous construction is not resolved in the expanding impulses we have continued with the study of geodesics in such a case. This has given us insights into their shift and refraction due to their interaction with gravitational impulses. We did this in the hope of reaching a better understanding of the path leading to the transformation between the continuous and distributional metric in the expanding case. However, this has not been accomplished yet and remains an open problem motivating our further research.

Besides the review part, where the majority of presented results have been independently recalculated, the original contribution is related to the behavior of free test particles interacting with the expanding gravitational impulses in the case generated by a snapped cosmic string. Using the procedures published in [29, 30], we have investigated the interaction of particles from the privileged family with $Z = \text{const}$ which seem to be reasonable candidates for continuous coordinate lines. In particular, we have focused on null geodesics belonging to this family. In conclusion, the thesis not only addresses specific theoretical challenges associated with impulsive gravitational waves, but also provides a foundation for our future research in this area.

Bibliography

[1] A. Einstein. Zur Allgemeinen Relativitätstheorie. *Sitzungsber. Preuss. Akad. Wiss. Berlin (Math. Phys.)*, 1915:778–786, 1915.

[2] C.W. Misner, K.S. Thorne, J.A. Wheeler, and D.I. Kaiser. *Gravitation*. Princeton University Press, 2017.

[3] R. M. Wald. *General relativity*. University of Chicago Press, Chicago, repr. edition, 2009.

[4] H. Stephani, D. Kramer, M. A. H. MacCallum, C. Hoenselaers, and E. Herlt. *Exact solutions of Einstein's field equations*. Cambridge monographs on mathematical physics. Cambridge University Press, 2003.

[5] J. B. Griffiths and J. Podolský. *Exact space-times in Einstein's general relativity*. Cambridge monographs on mathematical physics. Cambridge University Press, Cambridge, UK, 2009.

[6] J. Bičák. Selected Solutions of Einstein's Field Equations: Their role in general relativity and astrophysics. *Lecture Notes Physics*, 540:1–126, 2000.

[7] A. Friedmann. Über die Möglichkeit einer Welt mit konstanter negativer Krümmung des Raumes. *Zeitschrift für Physik*, 21:326–332, 1924.

[8] G. Lemaître. Un Univers homogène de masse constante et de rayon croissant rendant compte de la vitesse radiale des nébuleuses extra-galactiques. *Annales de la Société scientifique de Bruxelles*, 47:49–59, 1927.

[9] A. G. Walker. On Riemannian spaces with spherical symmetry about a line, and the conditions for isotropy in general relativity. *The Quarterly Journal of Mathematics*, 1:81–93, 1935.

[10] R. P. Kerr. Gravitational field of a spinning mass as an example of algebraically special metrics. *Physical Review Letters*, 11:237–238, 1963.

[11] J. Podolský. *Exact impulsive gravitational waves in spacetimes of constant curvature*, page 205–246. World Scientific, 2002.

[12] R. Penrose. *The geometry of impulsive gravitational waves*, pages 101–115. Clarendon Press, 1972.

[13] P. C. Aichelburg and R. U. Sexl. On the gravitational field of a massless particle. *General Relativity and Gravitation*, 2:303–312, 1971.

[14] Y. Nutku. Spherical shock waves in general relativity. *Physical Review D*, 44:3164–3168, 1991.

[15] J. Podolský and R. Steinbauer. Penrose junction conditions with Λ: geometric insights into low-regularity metrics for impulsive gravitational waves. *General Relativity and Gravitation*, 54:96, 2022.

[16] D. Kofroň, M. Karamazov, and R. Švarc. Interpretation of spacetimes with expanding impulsive gravitational waves generated by snapped cosmic strings. *Physical Review D*, 108:044059, 2023.

[17] J. Podolský and J. B. Griffiths. The collision and snapping of cosmic strings generating spherical impulsive gravitational waves. *Classical and Quantum Gravity*, 17:1401–1413, 2000.

[18] J. Podolský, C. Sämann, R. Steinbauer, and R. Švarc. The global existence, uniqueness and C^1-regularity of geodesics in nonexpanding impulsive gravitational waves. *Classical and Quantum Gravity*, 32:025003, 2014.

[19] J. Podolský, C. Sämann, R. Steinbauer, and R. Švarc. The global uniqueness and C^1-regularity of geodesics in expanding impulsive gravitational waves. *Classical and Quantum Gravity*, 33:195010, 2016.

[20] M. Kunzinger and R. Steinbauer. A Note on the Penrose junction conditions. *Classical and Quantum Gravity*, 16:1255–1264, 1999.

[21] J. Podolský and J. B. Griffiths. Expanding impulsive gravitational waves. *Classical and Quantum Gravity*, 16:2937, 1999.

[22] J. Bičák, C. Hoenselaers, and B. G. Schmidt. The Solutions of the Einstein Equations for Uniformly Accelerated Particles without Nodal Singularities. I. Freely Falling Particles in External Fields. *Proceedings of the Royal Society of London Series A*, 390:397–409, 1983.

[23] J. F. Colombeau. New generalized functions and multiplication of distributions. *North Holland, Amsterdam*, 1984.

[24] J. F. Colombeau. Elementary introduction to new generalized functions. *North Holland, Amsterdam*, 1985.

[25] M. Erlacher, E. Grosser. Inversion of a 'discontinuous coordinate transformation' in general relativity. *Applicable Analysis*, 90:1707–1728, 2011.

[26] A. F. Filippov. *Differential Equations with Discontinuous Righthand Sides*. Springer Dordrecht, 1988.

[27] R. Steinbauer. On the geometry of impulsive gravitational waves. *arXiv e-prints*, 2013.

[28] A. Lecke, R. Steinbauer, and R. Švarc. The regularity of geodesics in impulsive pp-waves. *General Relativity and Gravitation*, 46:1648, 2013.

[29] J. Podolský and R. Steinbauer. Geodesics in spacetimes with expanding impulsive gravitational waves. *Physical Review D*, 67:064013, 2003.

[30] J. Podolský and R. Švarc. Refraction of geodesics by impulsive spherical gravitational waves in constant-curvature spacetimes with a cosmological constant. *Physical Review D*, 81:124035, 2010.